The Plant Cell, Vol. 21: 3379–3396, October 2009, www.plantcell.org

Sfp-Type 4'-Phosphopantetheinyl Transferase Is Indispensable for Fungal Pathogenicity [W]

Ralf Horbach,[a,1] Alexander Graf,[a,2] Fabian Weihmann,[a] Luis Antelo,[b] Sebastian Mathea,[c] Johannes C. Liermann,[d] Till Opatz,[d] Eckhard Thines,[b] Jesús Aguirre,[e] and Holger B. Deising[a,3]

[a] Martin-Luther-Universität Halle-Wittenberg, Naturwissenschaftliche Fakultät III, Institut für Agrar und Ernährungswissenschaften, Phytopathologie und Pflanzenschutz, D-06099 Halle (Saale), Germany
[b] Institut für Biotechnologie und Wirkstoff-Forschung, D-67663 Kaiserslautern, Germany
[c] Max-Planck-Forschungsstelle für Enzymologie der Proteinfaltung, D-06120 Halle (Saale), Germany
[d] Institut für Organische Chemie, Universität Hamburg, D-20146 Hamburg, Germany
[e] Instituto de Fisiología Celular,Universidad Nacional Autónoma de México, 04510 Mexico, D.F., Mexico

In filamentous fungi, Sfp-type 4'-phosphopantetheinyl transferases (PPTases) activate enzymes involved in primary (α-aminoadipate reductase [AAR]) and secondary (polyketide synthases and nonribosomal peptide synthetases) metabolism. We cloned the PPTase gene *PPT1* of the maize anthracnose fungus *Colletotrichum graminicola* and generated PPTase-deficient mutants (Δ*ppt1*). Δ*ppt1* strains were auxotrophic for Lys, unable to synthesize siderophores, hypersensitive to reactive oxygen species, and unable to synthesize polyketides (PKs). A differential analysis of secondary metabolites produced by wild-type and Δ*ppt1* strains led to the identification of six novel PKs. Infection-related morphogenesis was affected in Δ*ppt1* strains. Rarely formed appressoria of Δ*ppt1* strains were nonmelanized and ruptured on intact plant. The hyphae of Δ*ppt1* strains colonized wounded maize (*Zea mays*) leaves but failed to generate necrotic anthracnose disease symptoms and were defective in asexual sporulation. To analyze the pleiotropic pathogenicity phenotype, we generated AAR-deficient mutants (Δ*aar1*) and employed a melanin-deficient mutant (M1.502). Results indicated that PPT1 activates enzymes required at defined stages of infection. Melanization is required for cell wall rigidity and appressorium function, and Lys supplied by the AAR1 pathway is essential for necrotrophic development. As PPTase-deficient mutants of *Magnaporthe oryzea* were also nonpathogenic, we conclude that PPTases represent a novel fungal pathogenicity factor.

INTRODUCTION

Secondary metabolism and virulence are closely linked traits in fungi attacking plants and mammals. Many of the structurally diverse secondary metabolites contributing to pathogenicity are polyketides (PKs) or nonribosomal peptides (NRPs), and this diversity is reflected by the large number of genes encoding polyketide synthases (PKSs) or nonribosomal peptide synthetases (NRPSs). For example, in *Cochliobolus heterostrophus*, the causal agent of Southern Leaf Blight of maize (*Zea mays*), 25 PKS- and 11 NRPS-coding genes have been identified (Kroken et al., 2003; Lee et al., 2005). In several *Colletotrichum* species and in the rice blast fungus *Magnaporthe oryzae*, PK-derived melanin is required for generation of turgor pressure in infection cells called appressoria and, thus, for pathogenicity (Howard et al., 1991; De Jong et al., 1997; Bechinger et al., 1999; Deising et al., 2000). Also, in fungi attacking humans (e.g., *Aspergillus fumigatus* and *Cryptococcus neoformans*), melanin contributes to virulence, presumably by quenching reactive oxygen species and protecting hyphae against human monocytes (Langfelder et al., 2003). In addition to melanin, toxins synthesized by PKSs determine fungal virulence on plants. The carbon chain of the host-selective T-toxin of *C. heterostrophus* is probably assembled by the action of two PKSs (Baker et al., 2006). A closely related pathogen, the Northern Leaf Blight fungus, *Cochliobolus carbonum*, produces the host-selective HC toxin, a cyclic tetrapeptide synthesized by a NRPS (Panaccione et al., 1992; Walton, 2006). Genes encoding other NRPS proteins (e.g., *NPS6* of *C. heterostrophus* and orthologs in different economically relevant plant pathogenic Ascomycota, such as *Cochliobolus miyabeanus*, *Gibberella zeae*, *Alternaria brassicicola*, and *M. oryzae*) are involved in siderophore synthesis and iron acquisition, tolerance to H_2O_2, and virulence (Oide et al., 2006; Hof et al., 2007). Siderophores are also pathogenicity factors in fungi infecting man (Schrettl et al., 2007). In addition to PKSs and NRPSs, bioinformatics approaches have recently revealed the existence of hybrid PKS-NRPS genes in several fungi. Interestingly, in the rice blast fungus *M. oryzae*, one of the PKS-NRPS genes, *ACE1*, acts as an avirulence gene, and the metabolite likely formed by the ACE1 enzyme elicits defense responses in rice cultivars

[1] Current address: Institut für Biotechnologie und Wirkstoff-Forschung, Erwin-Schrödinger-Str. 56, D-67663 Kaiserslautern, Germany.
[2] Current address: Department of Metabolic Biology, John Innes Centre, Norwich Research Park, Norwich NR4 7UH, UK.
[3] Address correspondence to holger.deising@landw.uni-halle.de.
The author responsible for distribution of materials integral to the findings presented in this article in accordance with the policy described in the Instructions for Authors (www.plantcell.org) is: Holger B. Deising (holger.deising@landw.uni-halle.de).
[W] Online version contains Web-only data.
www.plantcell.org/cgi/doi/10.1105/tpc.108.064188

carrying the Pi33 resistance gene (Fudal et al., 2007). Thus, a large body of literature indicates that PKs, NRPs, and PK-NRP hybrid molecules govern the interaction between pathogenic fungi and their hosts.

Despite the enormous chemical diversity in the secondary metabolites they synthesize, PKSs, NRPSs, and hybrid PKS-NRPSs share a common point of regulation. With the exception of type III PKSs, all of these enzymes require activation by 4'-phosphopantetheinylation at conserved Ser residues by an enzyme called 4'-phosphopantetheinyl transferase (PPTase). In yeast, three phosphopantetheinylated proteins (i.e., the cytoplasmic fatty acid synthase complex, a mitochondrial acyl carrier protein, and an α-aminoadipate reductase [AAR] involved in Lys biosynthesis) are known (Ehmann et al., 1999; Fichtlscherer et al., 2000). Different 4'-phosphopantetheinyl transferase (4'-PPTase) mutants are specifically affected in only one of these activities, with the other two remaining functional, indicating that specific 4'-PPTases exist in primary metabolism in *Saccharomyces cerevisiae* (Fichtlscherer et al., 2000). In the filamentous ascomycete *Aspergillus nidulans*, a single 4'-PPTase appears to regulate enzymes involved in both primary and secondary metabolism. A sound body of literature demonstrates that mutants deficient in the 4'-PPTase-encoding gene *npgA*/*cfwA* are Lys auxotrophs unable to synthesize several PK, including the conidiospore pigments and the mycotoxin sterigmatocystin, and NRPs such as penicillin and siderophores (Han and Han, 1993; Guzmán-de-Peña et al., 1998; Keszenman-Pereyra et al., 2003; Oberegger et al., 2003; Marquez-Fernandez et al., 2007). Like *A. nidulans*, other filamentous ascomycetes, such as *A. fumigatus*, *M. orzyae*, *G. zeae*, and *Neurospora crassa*, have single-copy *cfwA*/*npgA* homologs (Marquez-Fernandez et al., 2007).

The contribution of PKS-, NRPS-, and PKS-NRPS-derived secondary metabolites to fungal virulence has been demonstrated in several pathogens (Rasmussen and Hanau, 1989; Henson et al., 1999; Oide et al., 2006; Greenshields et al., 2007; Steiner and Oerke, 2007; Collemare et al., 2008), indirectly arguing that PPTases may play a central role in the infection process. However, no data directly demonstrate that PPTases are required for pathogenicity on plants, and the role of individual enzymes that require 4'-phosphopantetheinylation has not been analyzed in different stages of the infection process.

Mootz et al. (2002) deleted the PPTase-encoding *lys5* gene of *S. cerevisiae* and demonstrated that Lys prototrophy was restored by complementation with genes from *Bacillus* sp encoding Sfp- and Gsp-type PPTases. The *Schizosaccharomyces pombe lys7* and the *A. nidulans npgA* gene also complemented the *lys5* deletion and have thereby been functionally characterized as PPTase genes. Mootz et al. (2002) suggested that this functional complementation system could allow for the simple cloning of 4'-PPTase genes from cDNA libraries of diverse origin. Taking advantage of this strategy, we cloned the Sfp-type PPTase gene *PPT1* of the maize pathogen *Colletotrichum graminicola*, the causal agent of leaf anthracnose and stalk rot (Bergstrom and Nicholson, 1999). Targeted mutagenesis revealed that *PPT1* is required for Lys prototrophy, acquisition of iron, tolerance to reactive oxygen intermediates, formation and melanization of infection cells, invasion of intact maize leaves, switch to necrotrophic development, formation of anthracnose leaf symptoms, and asexual sporulation. Infection assays performed with melanin-deficient UV mutants (Rasmussen and Hanau, 1989) and with AAR-deficient mutants produced by targeted gene deletion allowed us to dissect the pleiotropic effects of this enzyme and to define the infection stages at which enzymes activated by PPT1 are required for pathogenicity. Furthermore, deletion of the *PPT1* homolog in *M. oryzae* confirmed the role of PPT1 in pathogenicity in another pathosystem. Thus, *PPT1* is a novel fungal pathogenicity gene and may represent a novel multifunctional antifungal target.

RESULTS

Complementation of Yeast Mutant Δ*lys5* and 4'-Phosphopantetheinylation of a PKS Fragment Demonstrate the PPTase Function of *PPT1* of *C. graminicola*

To clone the *C. graminicola* PPTase gene by complementation of the PPTase-deficient yeast mutant strain BO4421 (Δ*lys5*), which is auxotrophic for Lys, a cDNA library was constructed from melanized saprophytic mycelium. The binary vector pAG300 allowed expression of *C. graminicola* cDNAs in yeast under control of the constitutive yeast *ADH1* promoter. As a positive control, the yeast Δ*lys5* strain was complemented with the *A. nidulans* PPTase gene *cfwA* (Figure 1A, T_{cfwA}). Of 4.5 million yeast transformants harboring *C. graminicola* cDNA, eight were prototrophic for Lys (T_{AG1} to T_{AG8}) (Figure 1A, T_{AG2} and T_{AG5}), indicating the presence of a functional PPTase. In contrast with the Lys prototrophic reference strain BY4741 and transformants T_{AG2}, T_{AG5}, and T_{cfwA}, the *Δlys5* strain BO4421 and strain BO4421 transformed with the empty vector (T_{pAG300}) were auxotrophic for Lys (Figure 1A).

In liquid culture, the *S. cerevisiae* wild-type strain BY4741 (see Supplemental Figure 1 online, black line) and the transformants T_{cfwA} (see Supplemental Figure 1 online, green line), T_{AG2}, and T_{AG5} (see Supplemental Figure 1 online, blue lines) showed similar growth rates. Doubling times were 71 min for BY4741, 70 min for T_{cfwA} and T_{AG5}, and 67 min for T_{AG2}. However, initiation of exponential growth of BY4741 lagged ~120 min behind transformants T_{AG2} and T_{AG5} and ~70 min behind T_{cfwA}. In the absence of Lys, the Δ*lys5* strain BO4421 and BO4421 transformed with the empty vector (T_{pAG300}) did not grow (see Supplemental Figure 1 online, gray lines).

The sequences of the cDNAs expressed in all transformants prototrophic for Lys were identical and showed significant similarity with those of other fungal PPTase genes in BLAST analyses, as indicated by e-values (*M. oryzae* $2e^{-91}$, *G. zeae* $5e^{-75}$, *N. crassa* $1e^{-64}$, and *A. nidulans* $4e^{-34}$). Based on functional complementation of the Δ*lys5* mutants and sequence homology, we designated *PPT1* to the *C. graminicola* PPTase gene. This gene consists of 1113 bp and contains an intron of 178 bp, starting at position 85 from the beginning of the start codon. The intron is flanked by characteristic 3′GT and 5′AG splicing signals and contains a typical branching point motif (CTGAC). The deduced protein (PPT1) consists of 311 amino acids and has a

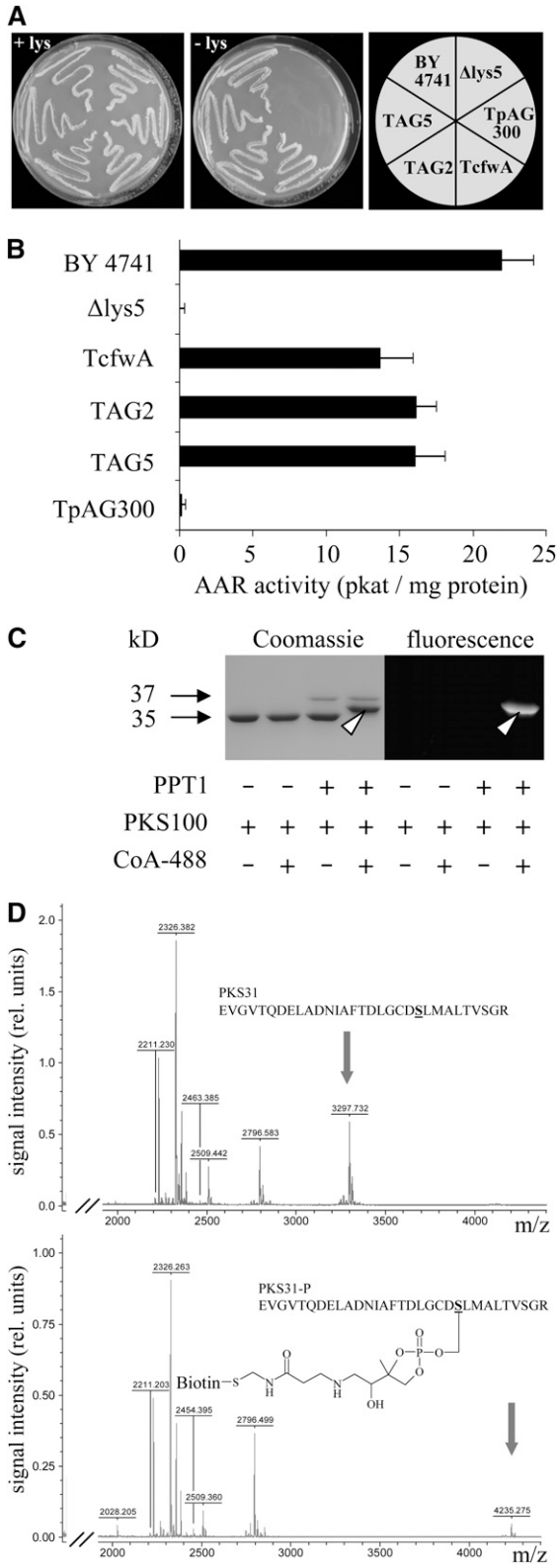

Figure 1. Cloning of the *C. graminicola* PPTase Gene by Complementation of the *S. cerevisiae* Δ*lys5* Mutant, Confirmation of AAR Activity, and 4'-Phosphopantetheinylation of a PKS Fragment.

calculated relative molecular mass (M_r) of 34.854. PPT1 of *C. graminicola* is 54 and 50% identical to the PPTases of *M. oryzae* and *G. zeae*, respectively, and 32% identical to the *A. nidulans* protein CfwA. Remarkably, PPT1 of *C. graminicola* is only 20% identical to *S. cerevisiae* Lys5p.

As activation of AAR strictly depends on 4'-phosphopantetheinylation, AAR activity can be taken as indirect evidence for PPTase activity. AAR activity was detected in cell-free extracts of wild-type strain BY4741, and transformants T_{cfwA}, T_{AG2}, and T_{AG5}, but not in extracts of the Δ*lys5* mutant BO4421 and transformant T_{pAG300} (Figure 1B). Furthermore, 4'-phosphopantetheinylation of a *C. graminicola* PKS fragment containing a conserved Ser (amino acids 1618 to 1717 of PKS1, see below) demonstrated PPTase activity of PPT1 directly (Figure 1C). 4'-Phosphopantetheinylation of the GST-PKS100 fragment only occurred if the reaction mixture contained both affinity-purified recombinant proteins, for example, the 37.1-kD $(His)_6$-PPT1 [consisting of the 34.9-kD PPTase and a $(His)_6$-tag accounting for 2.2 kD] and the 37.4-kD GST-PKS100 (consisting of the 100–amino acid 10.9-kD PKS100 fragment and the 26.5-kD glutathione *S*-transferase [GST] tag), as well as CoA conjugated to fluorophore ATTO 488. This was indicated by an electrophoretic mobility shift in SDS-PAGE (Figure 1C, Coomassie-stained gel, arrowhead). As expected, only the shifted band representing the 4'-phosphopantetheinylated GST-PKS100 fragment fluoresced upon irradiation at 473 nm, due to the fluorophore being linked to the 4'-phosphopantetheinyl residue (Figure 1C, fluorescence image, arrowhead).

Matrix-assisted laser-desorption ionization time of flight mass spectrometry (MALDI-TOF MS) analysis was used to further demonstrate the covalent link between the 4'-phosphopantetheinyl residue and the GST-PKS100 target protein. The 4'-phosphopantetheinylated and the non-4'-phosphopantetheinylated

(A) The reference yeast strain BY4741 and Δ*lys5* transformants T_{cfwA}, T_{AG2}, and T_{AG5} expressing PPTase cDNAs from *A. nidulans* and *C. graminicola*, respectively, were able to grow on medium lacking Lys (-lys). By contrast, Δ*lys5* or the Δ*lys5* transformant containing the empty expression vector (T_{pAG300}) were auxotroph for Lys. All yeast strains grew on medium amended with Lys (+lys).

(B) AAR activity was detectable in cell-free extracts from strains BY4741, T_{cfwA}, T_{AG2}, and T_{AG5} but not in extracts from the Δ*lys5* strain and T_{pAG300}. Three independent experiments were performed; bars represent SD.

(C) 4'-phosphopantetheinylation of a 100–amino acid *C. graminicola* PKS1 fragment (PKS100) fused to GST, as indicated by a band shift in Coomassie blue–stained gels and by fluorescence (arrowheads), only occurred when affinity-purified PPT1 and PKS100 and fluorochrome ATTO488-conjugated CoA were present in the reaction mixture.

(D) Affinity-purified PKS100 was incubated with PPT1 in the absence (top) or presence (bottom) of biotin-conjugated CoA. After tryptic digest, MALDI-TOF MS analysis of a 31–amino acid peptide (PKS31) containing the conserved DSL phosphopantetheinylation site showed a mass shift only when biotin-conjugated CoA was present in the reaction mixture. Arrows indicate peaks corresponding to PKS31 (calculated *m/z* = 3299.645, measured *m/z* = 3297.732, error of 0.058%) and the phosphopantetheinylated PKS31-P (calculated *m/z* = 4237.705, measured *m/z* = 4235.275, error of 0.057%).

fragments were tryptically digested, and shifts in the molecular mass of the resulting fragments were analyzed. The affinity-purified GST-PKS100 fragment was tryptically digested, and a 31–amino acid fragment contained a conserved Ser at position 22 (Figure 1D, PKS31, S underlined) and the DSL consensus signal for 4'-phosphopantetheinylation (Mofid et al., 2002). Indeed, the mass-to-charge (*m/z*) values of the non-4'-phosphopantetheinylated and the 4'-phosphopantetheinylated 31–amino acid fragments were 3297.732 and 4235.275, respectively (Figure 1D, arrows). The difference exactly corresponds to the mass of the biotinylated 4'-phosphopantetheinyl residue.

Thus, yeast complementation and biochemical data show that PPT1 of *C. graminicola* is capable of 4'-phosphopantetheinylating and activating proteins containing a conserved Ser. These data are in agreement with reports from other Sfp-type PPTases, including *A. nidulans* CfwA, which is required for activation of AAR, PKSs, and NRPSs (Neville et al., 2005; Yin et al., 2005; Marquez-Fernandez et al., 2007).

PPT1 Mutants of *C. graminicola* Are Auxotrophic for Lys, Nonmelanized, Unable to Synthesize PKS- and NRPS-Dependent Secondary Metabolites, Unable to Grow under Iron-Limiting Conditions, and Hypersensitive to Reactive Oxygen Species

To functionally characterize the *PPT1* gene of *C. graminicola*, targeted mutagenesis was performed (see Supplemental Figure 2 online). In the knockout vector, the 182-bp *Eco*81I fragment of the gene was replaced by a 2.6-kb fragment carrying the *Escherichia coli* hygromycin phosphotransferase gene (*hph*) (see Supplemental Figure 2A online). As indicated by DNA gel blot analyses performed with *Pst*I-digested genomic DNA, the 1597-bp wild-type band had been replaced by the 2279-bp fragment in all independent knockout strains (*Δppt1*; KO). Transformants with ectopically integrated KO vector (ect.) showed the 2279-bp band in addition to the 1597-bp wild-type band (see Supplemental Figure 2B online). To confirm gene inactivation at the transcript level, RT-PCR experiments were performed with primers specific for *PPT1* transcripts, using total RNA from the wild-type and three independent KO strains. Primers corresponding to transcripts of the constitutively expressed *C. graminicola CHSII* gene (Werner et al., 2007) were used as a control (see Supplemental Figure 2C online). As expected, the 380-bp *CHSII* fragment was amplified from RNA from wild-type and KO strains, but the 936-bp *C. graminicola PPT1* fragment only occurred when RNA from the wild-type strain was used as a template (see Supplemental Figure 2C online). These data confirm the successful targeted mutagenesis of *PPT1*.

Hyphal pigmentation and growth assays on Lys- and iron-limited synthetic minimal medium indicated the requirement of PPT1 for activation of AAR, PKSs, and NRPSs (Figure 2). The wild-type strain and the transformants with ectopic integration of the KO vector (ect.), but not the KO strain, were able to grow on Lys-deficient synthetic minimal medium (Figure 2A, SMM). Although slightly reduced growth rates sometimes occurred in ectopic transformants, these results fully support the yeast complementation assays (Figure 1A; see Supplemental Figure 1A online). As expected, supplementing the medium with Lys rescued the growth defect of *Δppt1* strains but was insufficient to restore melanization (Figure 2A, SMM + lys). Likewise, on rich media such as synthetic complete medium (Figure 2A, SCM) or potato dextrose agar (Figure 2A, PDA), *Δppt1* strains were able to grow but failed to melanize. On potato dextrose agar, *Δppt1* strains appeared grayish due to the color of the medium. These data suggest that PPT1 is required for activating both AAR and PKS.

Siderophores are NRPs that mediate iron uptake and growth under iron-limiting conditions (Antelo et al., 2006; Haas et al., 2008). Addition of the iron chelator bathophenanthroline-disulfonate to synthetic complete medium caused complete growth inhibition of the *Δppt1* strains, but the wild-type strain and ectopic transformants were able to grow (Figure 2A, SCM + BPS). Growth of the KO strains was restored by adding the siderophores desferri-ferrichrome (see Supplemental Figure 3 online) or desferri-coprogen (cop) (Figure 2A, SCM + BPS + cop). Indeed, HPLC-MS analyses of culture filtrates of the wild-type strain showed that *C. graminicola* secreted the siderophores coprogen B (Figure 2B, blue line) and 2-*N*-methylcoprogen B (Figure 2B, black line) under iron-limiting conditions; culture filtrates of *Δppt1* strains did not contain any siderophore (Figure 2B, red line). Furthermore, only the wild-type strain but not the mutants contained the intracellular siderophore ferricrocin (see Supplemental Figure 4 online). These results are in agreement with reports of growth defects of siderophore-deficient mutants of *G. zeae* and *C. heterostrophus* under iron-limiting conditions (Oide et al., 2006; Greenshields et al., 2007). Chelation of iron is required to prevent an increase in the levels of reactive oxygen species (Haas et al., 2008). As expected, growth of *Δppt1* strains was severely inhibited on media containing H_2O_2 or rose bengal, which produces singlet oxygen radicals when illuminated (Figure 2A, PDA + H_2O_2 and PDA + RB).

Differential metabolite analyses in culture filtrates revealed that several secondary metabolites were formed by the wild type but not by the *Δppt1* strains (Figure 3). In addition to the extracellular NRPs coprogen B and 2-*N*-methylcoprogen B (Figure 2B), the intracellular iron storage NRP ferricrocin was detected in hyphal extracts (see Supplemental Figure 4 online). Furthermore, we identified six novel fungal metabolites using HPLC-MS and nuclear magnetic resonance (NMR) spectrometry, including two pyrones (colletopyrone B and C), two anthraquinones (colletoquinone A and B), a 10-hydroxyanthrone (colletoanthrone A), and an 11-membered macrolactone (colletolactone A) (Figure 3; see Supplemental Figure 5 Supplemental Tables 1 to 4 online). In addition, the compounds orcinol, tryptophol, indole-3-acetic acid, himanimide C, and 2-phenylethanol have been found in culture filtrates of the wild-type strain (Supplemental Figure 5 online). Interestingly, tyrosol, which has been described as a PK in the fungus *Beauveria bassiana* (Fuganti et al., 1996), was present in culture filtrates of both wild-type and *Δppt1* strains, suggesting that tyrosol is synthesized via the shikimate pathway.

Toxicity assays were performed by applying 5-μL droplets containing all of the purified compounds individually at a concentration of 1 μg/μL onto wounded and nonwounded maize leaves. One, two, and three days after application of the secondary metabolites, leaves were macroscopically investigated

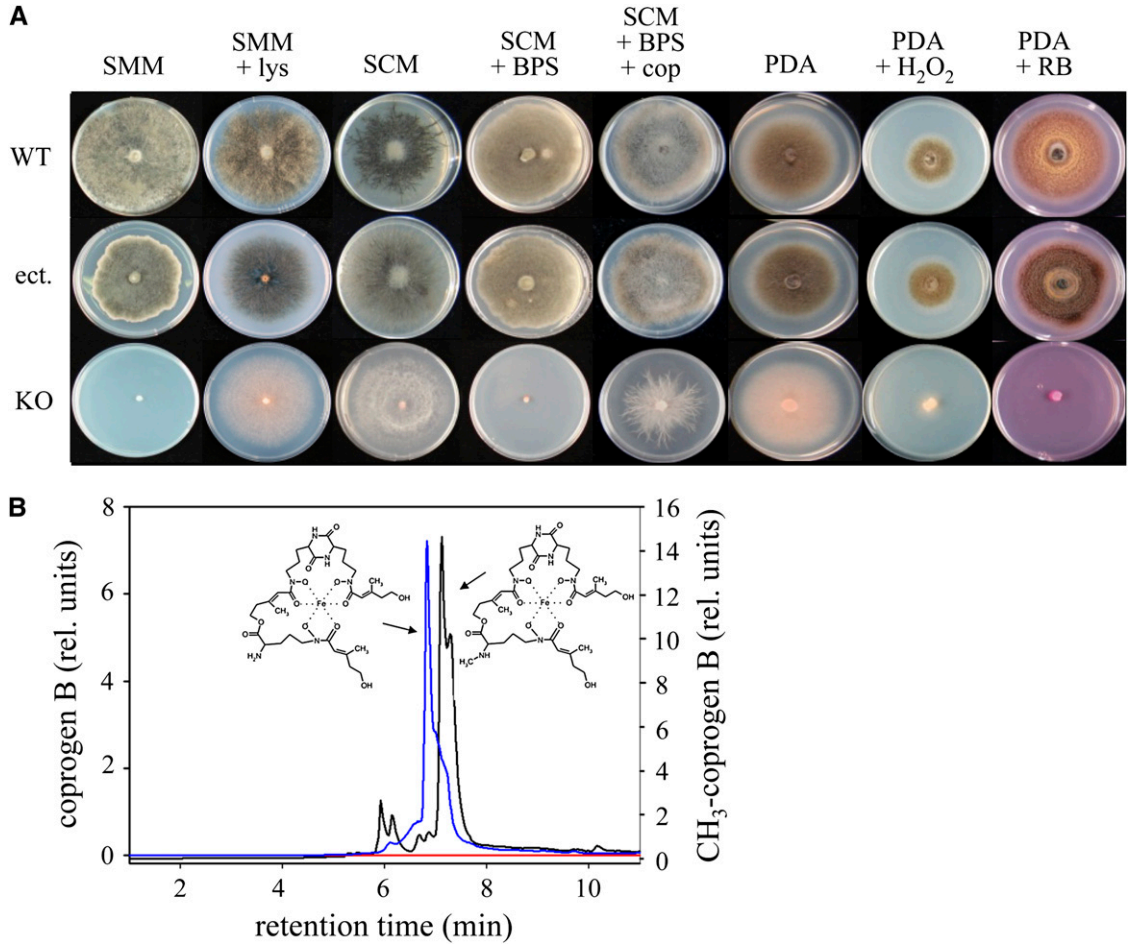

Figure 2. Growth Assays and Formation of Siderophores.

(A) In comparison with the wild-type strain and a strain carrying the ectopically integrated knockout vector (ect.), the KO strain is unable to synthesize melanin or to grow under iron-depleting conditions and is hypersensitive to reactive oxygen species. SMM, synthetic minimal medium; SCM, synthetic complete medium; BPS, bathophenanthroline-disulfonate; cop, desferri-coprogen; PDA, potato dextrose agar; RB, rose bengal.

(B) Analysis of siderophores formed by wild-type and *Δppt1* strains. HPLC profiles of culture filtrates indicate that the wild-type strain secretes coprogen B (blue line) and 2-*N*-methylcoprogen B (black line) into the culture medium. *Δppt1* strains do not secrete any siderophores (red line).

for the occurrence of necroses and microscopically for the occurrence of cell wall or whole-cell fluorescence under UV excitation. None of the compounds produced in liquid cultures caused cell death or autofluorescence of whole cells or cell walls under these conditions, suggesting that they are not phytotoxic.

Taken together, these data show that the Sfp-type PPTase PPT1 plays a central role in Lys biosynthesis and synthesis of secondary metabolites required for pigmentation, acquisition of iron, and tolerance to oxidative stress in *C. graminicola*.

PPT1 of *C. graminicola* Is Required for Asexual Sporulation, Germ Tube Morphology, and Differentiation of Functional Appressoria

Marquez-Fernandez et al. (2007) demonstrated that severe asexual sporulation defects occurred in PPTase-deficient *cfwA* mutants of *A. nidulans*. To analyze the effect of *PPT1* of *C. graminicola* on the size and morphology of oval and falcate conidia, wild-type and *Δppt1* strains were allowed to sporulate in liquid complete medium. Conidia of the *Δppt1* strains were smaller than wild-type conidia and showed drastic morphological defects (i.e., small conidia had round to spherical shapes and larger spores had central protrusions or round poles; Figure 4A). Interestingly, germination rates of mutant and wild-type conidia were similar on different hydrophobic substrata (i.e., polyester sheets, onion [*Allium cepa* cv Grano] epidermis, and maize surface; Figure 4B). However, germ tubes of *Δppt1* strains frequently branched (Figure 4C).

Differentiation of melanized functional infection cells, such as appressoria or hyphopodia, is essential for pathogenicity of *C. graminicola* (Rasmussen and Hanau, 1989; Deising et al., 2000; Werner et al., 2007). To investigate the role of *PPT1* in

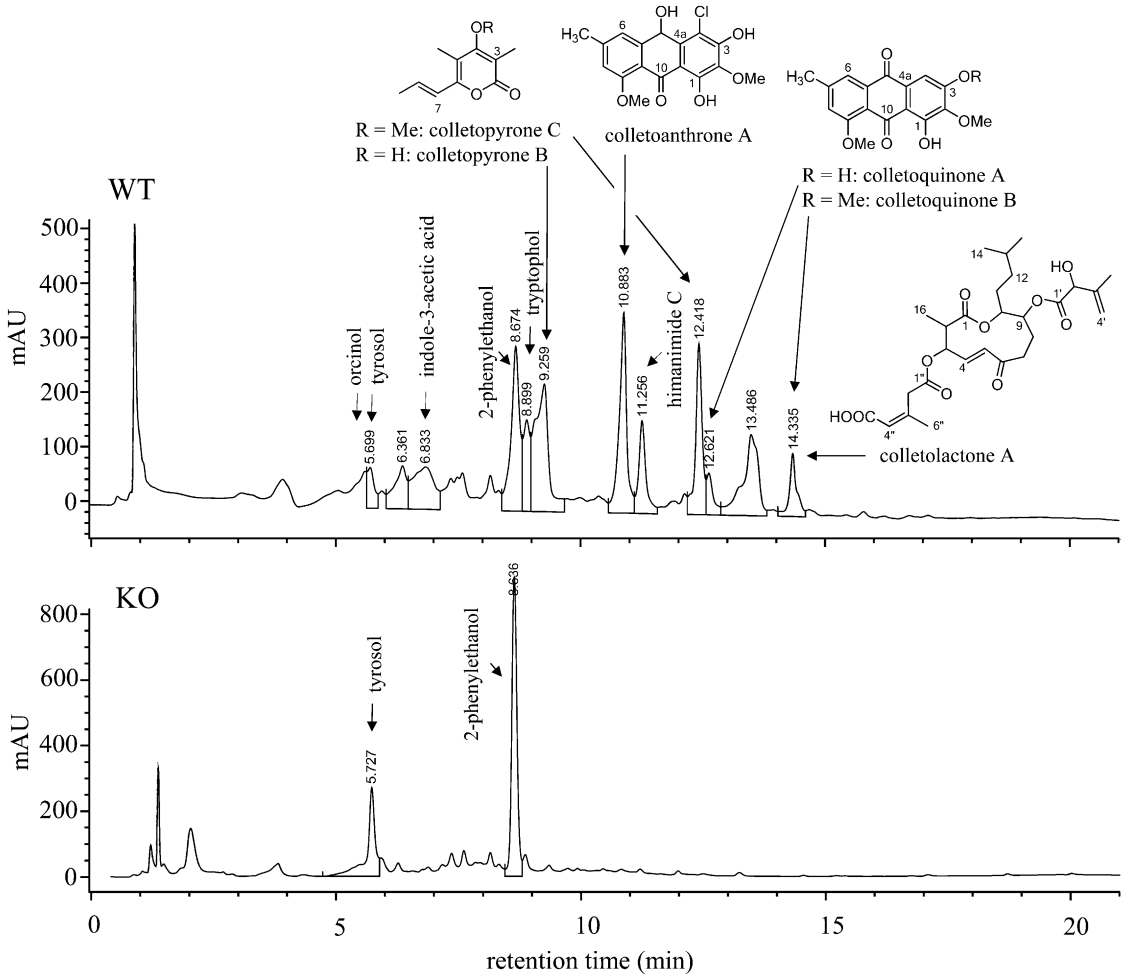

Figure 3. HPLC Profiles and Secondary Metabolites Identified in Culture Filtrates of Wild-Type and *Δppt1* (KO) Strains.

Chemical structures of orcinol, tryptophol, colletopyrone B and C, colletoanthrone A, colletoquinone A and B, and colletolactone A were identified by NMR. Tyrosol, indole-3-acetate, phenylethanol, and himanimide C were identified by employing reference data (HPLC retention time, UV, and mass spectra) from the IBWF compound library. The detection wavelength was 210 nm.

appressorium differentiation and melanization, wild-type and *Δppt1* conidia were inoculated onto artificial and natural hydrophobic substrata (i.e., polyester, onion epidermal layers, and maize leaf surfaces; Figure 5). While the wild-type strain germinated and efficiently formed appressoria on all hydrophobic surfaces, *Δppt1* strains showed severely reduced rates of appressorium formation (Figure 5A), although they had no defects in germination rates (Figure 4B). As expected, wild-type appressoria were strongly melanized (Figure 5B, asterisk), but infection cells of *Δppt1* strains lacked melanization (Figure 5C, arrowhead). To determine appressorium function, penetration rates on maize leaves were quantified. While penetration rates of wild-type appressoria were 86% ± 6% in laboratory experiments with maize leaf segments, invasion of epidermal cells by those rarely formed nonmelanized appressoria of *Δppt1* strains was not observed. Surprisingly, microscopy analyses revealed that most nonmelanized appressoria of *Δppt1* strains ruptured on the leaf surface, as indicated by the spontaneous release of cytoplasm (cf. Figures 5D and 5E, arrows). By contrast, we never observed bursting of wild-type appressoria. These data suggest that a PKS activated by PPT1 is involved in appressorial melanization and cell wall stability.

PPT1 Is Expressed at All Stages of Pathogenesis

The role of *PPT1* in both primary and secondary metabolism suggests that this gene would be expressed at all stages of pathogenesis. As infection structure differentiation and leaf infection do not occur perfectly synchronously, RT-PCR experiments do not provide information on *PPT1* expression in individual infection structures. Therefore, we analyzed expression of this gene during the infection process on leaves of the host plant, maize, and on epidermal layers of the alternate host, onion, using a *C. graminicola* transformant carrying a *PPT1*:enhanced green

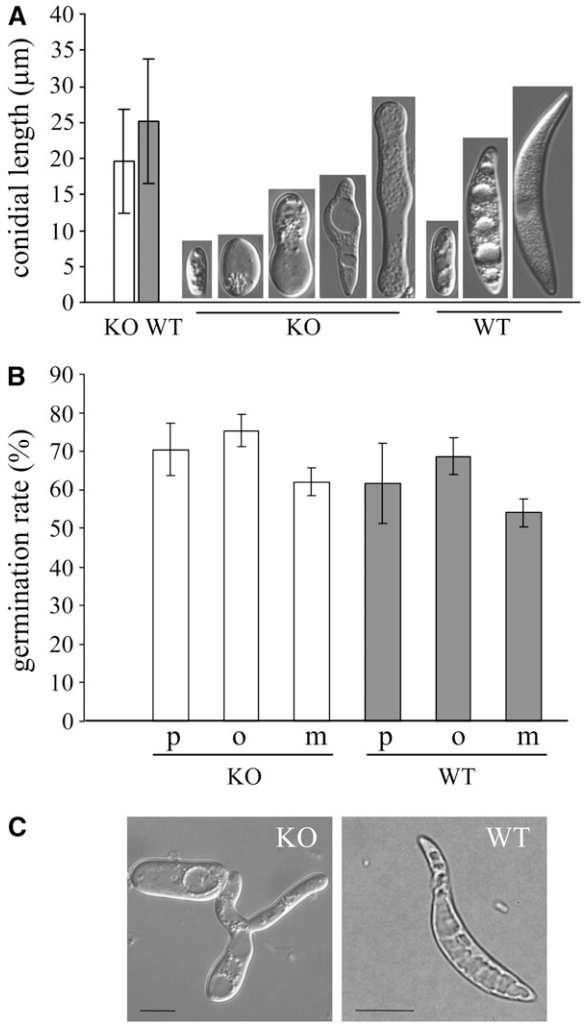

Figure 4. Formation of Asexual Spores.

(A) Size and shape of conidia formed by wild-type and *Δppt1* (KO) strains in liquid medium. Bars represent ± SD (n = 300). Conidial lengths of wild-type and KO strains differed significantly from each other ($P < 0.05$).
(B) Comparison of germination rates of conidia of KO strains (white columns) and the wild type (gray columns) on different hydrophobic substrata. p, polyester sheets; o, onion epidermis; m, maize surface. Bars represent ± SD (n = 600, $P > 0.05$).
(C) Germlings of a KO strain and the wild type. Note the branching of the germ tube of the KO strain. Bars = 10 µm.

fluorescent protein (*eGFP*) fusion under the control of the native *PPT1* promoter (Figure 6). Preliminary experiments had shown that virulence was not affected in this transformant. In both host backgrounds, infection structure formation was comparable. Conidia (arrowheads) had germinated and differentiated appressoria (arrow) by 24 h after inoculation (HAI), and biotrophic infection vesicles and thick primary hyphae had formed by 32 and 48 HAI, respectively (arrows). Thin secondary hyphae, indicative of necrotrophic development, were visible at 72 HAI (arrows), and newly formed conidia (arrows) were present at 120 HAI. GFP fluorescence was observed in all fungal structures formed (i.e., in conidia, germ tubes, and appressoria differentiated on the plant cuticle) and in biotrophic and necrotrophic hyphae formed in planta. These data indicate that *PPT1* was expressed at all stages of pathogenesis.

PPT1 Is Indispensable for Pathogenicity and Symptom Formation but Not for Growth in Planta

As *PPT1* is essential for siderophore and melanin biosynthesis, both of which represent pathogenicity or virulence determinants in plant pathogenic fungi (Rasmussen and Hanau, 1989;

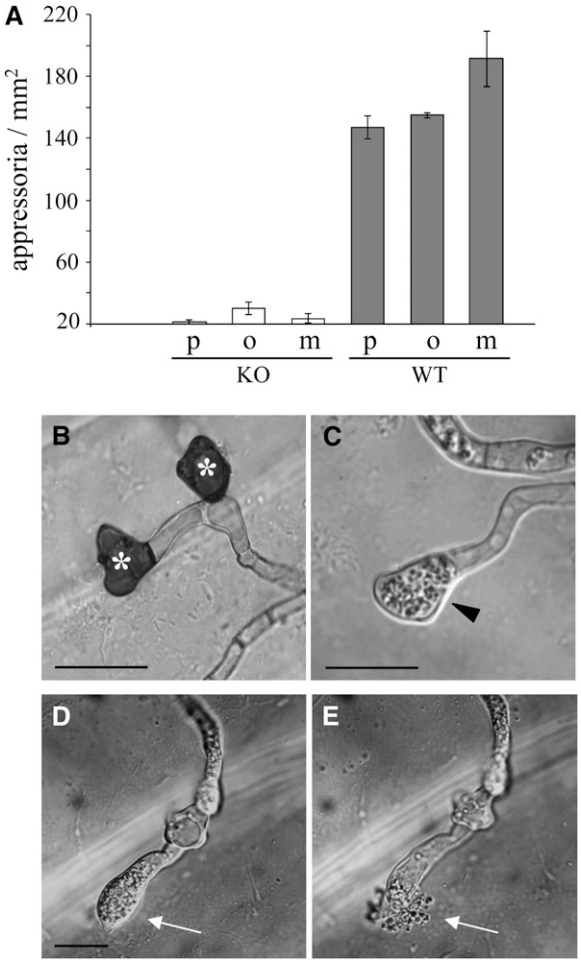

Figure 5. *Δppt1* (KO) Strains Are Unable to Differentiate Functional Appressoria.

(A) In contrast with the wild-type strain (gray columns), KO strains (white columns) formed significantly lower numbers of appressoria on hydrophobic substrata ($P < 0.05$). p, polyester sheets; o, onion epidermis; m, maize surface. Three independent experiments were performed (total number of fungal structures counted = 1842). Bars represent ± SD.
(B) Melanized wild-type appressoria (asterisks) formed on onion surface.
(C) Appressoria of KO strain (arrowhead) lacked melanization.
(D) and **(E)** Bursting appressorium and cytoplasm release from a KO strain (arrows, compare **[D]** and **[E]**). Bars = 10 µm.

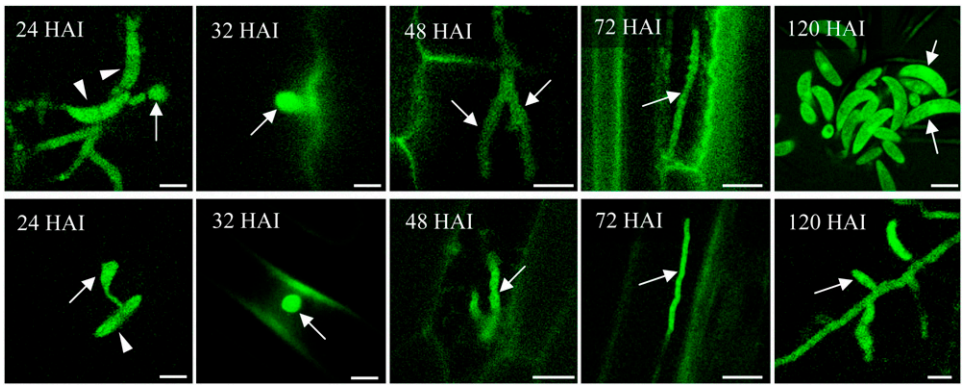

Figure 6. Expression of *PPT1* during Pathogenic Development of *C. graminicola*.

Expression of the *PPT1*:*eGFP* fusion in infected maize (top row) and onion (bottom row). By 24 HAI, conidia (arrowheads) had formed appressoria (arrows) on the plant surface. At 32, 48, 72, and 120 HAI, infection vesicles, primary hyphae, secondary hyphae, and newly formed conidia had formed, respectively, as indicated by arrows. GFP fluorescence is visible in all infection structures formed. Bars = 10 μm.

Nosanchuk and Casadevall, 2003; Greenshields et al., 2007; Hof et al., 2007; Haas et al., 2008), we analyzed the role of this gene in pathogenicity on maize leaves (Figure 7). When inoculated onto nonwounded leaves, the wild-type strain, but not the *Δppt1* strains, was able to cause leaf anthracnose disease symptoms (Figure 7A, WT and KO). Complementation of the *Δppt1* strains with the *PPT1* gene under control of the native promoter fully rescued growth defects on minimal medium lacking Lys (see Supplemental Figure 6 online), and complemented *Δppt1* strains (CP) regained full virulence on intact maize leaves (Figure 7A, KO and CP).

Melanin-deficient mutants of *C. graminicola* obtained after UV irradiation were impaired in host cell penetration, but lesion formation was restored when wounded leaves were inoculated with conidia of these mutants (Rasmussen and Hanau, 1989). To analyze whether the nonpathogenicity of *Δppt1* strains was only due to defects in melanization, we compared virulence of *C. graminicola* wild-type and *Δppt1* strains on wounded leaf segments (Figure 7B). At 6 d after inoculation (DAI), the wild-type strain caused severe anthracnose symptoms indicative of necrotic tissue; however, only minor chloroses but no typical anthracnose disease symptoms occurred after inoculation with the *Δppt1* strains (Figure 7B, WT and KO).

Interestingly, microscopy inspection of infection sites showed that the *Δppt1* strains were able to colonize the host tissue. At 2 DAI, both wild-type and *Δppt1* strains showed spreading growth and efficiently penetrated anticlinal plant cell walls (Figure 7C, arrows). In both wild-type and *Δppt1* strains, hyphal swellings reminiscent of inconspicuous appressoria were formed prior to penetration, which often occurred through plasmodesmata (Figure 7C, arrowhead). Massive colonization of leaves by both strains was observed at 4 DAI, and at 6 DAI, the wild-type strain had formed acervuli with conidia (Figure 7C, arrow) and melanized setae (Figure 7C, arrowhead). Although *Δppt1* strains were able to grow in the host tissue, they were arrested when initials of acervuli formed (Figure 7B, arrow) and exhibited major defects in conidiation. At 6 DAI, 3×10^5 and 7×10^5 conidia were recovered from nonwounded and wounded leaves infected by the wild-type strain, respectively; 0.3×10^4 and 3×10^4 were isolated from nonwounded and wounded *Δppt1*-infected leaves, respectively (Figure 7D).

To quantify pathogenic development of wild-type and *Δppt1* strains in wounded and nonwounded host leaves, quantitative PCR was performed using primers specific for the glyceraldehyde-3-phosphate dehydrogenase gene of *C. graminicola* (Figure 7E). The wild-type strain developed hyphae in both wounded and nonwounded leaves, with minor differences in the amount of fungal DNA, taken as an indicator of fungal biomass. The switch to necrotrophic development occurred at ~72 HAI, and massive growth of the wild-type strain was observed thereafter in both wounded and nonwounded leaves (cf. 72 and 120 HAI). By contrast, the *Δppt1* strains formed hyphae only in wounded but not in intact leaves. Significant development of the *Δppt1* strains was evident in wounded leaves, although the amount of DNA was only approximately half that of the wild-type strain on wounded but about two-thirds of the wild type on nonwounded leaves at 120 HAI (Figure 7E). Comparisons of fungal mass and symptom intensity (Figure 7B) suggest that it is unlikely that insufficient fungal mass would account for lack of necroses in leaves inoculated with the *Δppt1* strains. Thus, inactivation of the *PPT1* gene drastically diminished pathogenic development, but in planta growth of the *Δppt1* strains was reminiscent of an endophytic lifestyle.

To address the question of whether PPTase is a pathogenicity factor also in other plant pathogenic fungi, the *PPT1* gene was deleted in strain 70-15 of the rice blast fungus *M. oryzae*. The *Magnaporthe* genome (Dean et al., 2005) contains a single-copy PPTase gene. Replacement of *PPT1* by a hygromycin resistance cassette was performed by transforming conidia of *M. oryzae* with a KO construct consisting of the *hph* cassette flanked by ~1 kb of 5′- and 3′-flanks of the *PPT1* gene (see Supplemental Figure 7 online). Successful deletion was confirmed by DNA gel blots (see Supplemental Figure 7 online). Two independent *Δppt1* strains of *M. oryzae* (Figure 8, KO) and one strain carrying

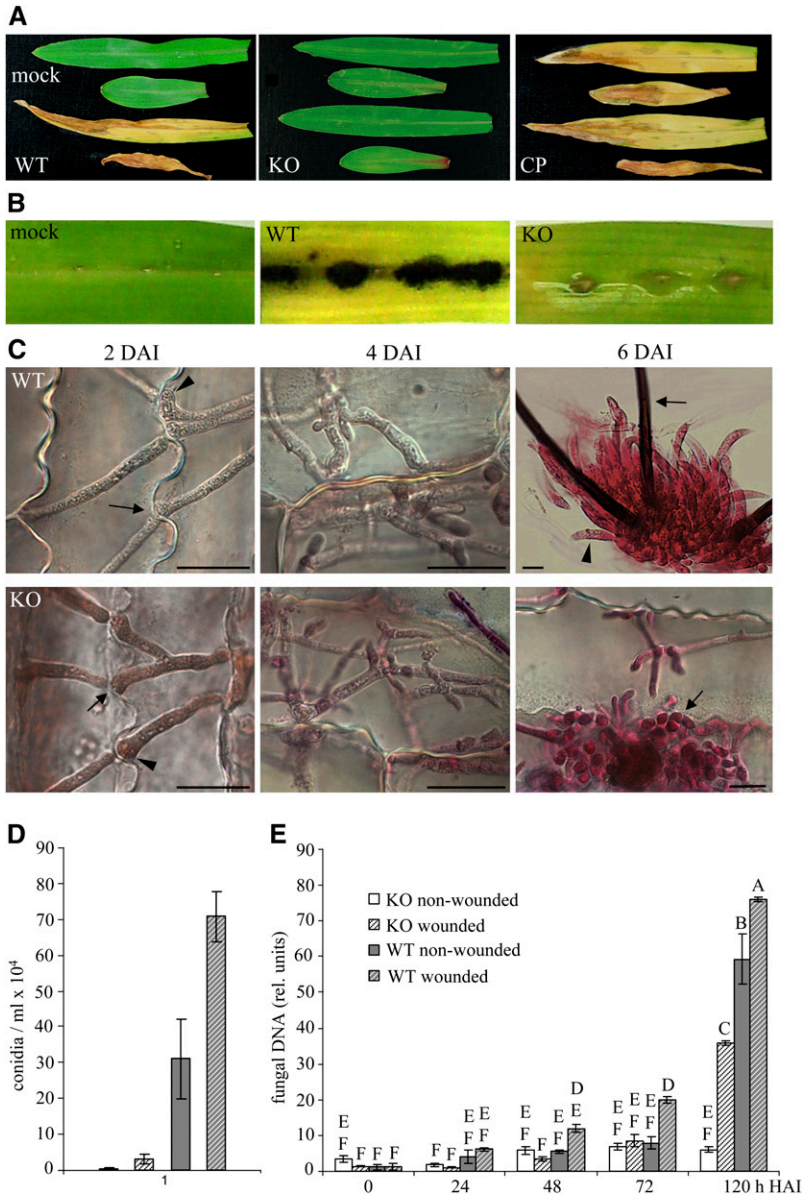

Figure 7. *Δppt1* Strains Are Nonpathogenic and Have Defects in Asexual Sporulation but Can Colonize Maize Leaf Tissue.

(A) Plant infection assays showed that the wild type, but not a representative *Δppt1* (KO) strain, caused anthracnose disease symptoms. Mock inoculation was performed with sterile 0.01% (v/v) Tween 20. In KO strains complemented with the *PPT1* gene (CP), full virulence on intact leaves was restored.

(B) Macroscopy evaluation of symptom development at 6 DAI on wounded leaves inoculated with the wild type and a KO strain; mock-inoculated leaves served as control.

(C) Micrographs of wounded leaves inoculated with the wild type and a representative KO strain showing fungal in planta development over 6 DAI. Black arrows indicate hyphae penetrating anticlinal plant cell walls at 2 DAI, and the arrowhead indicates a hyphal appressorium-like structure at the site of penetration; at 4 DAI, epidermal cells were colonized by wild type and the *Δppt1* strain; at 6 DAI, acervuli with conidia (arrowhead) and setae (arrow) were formed by the wild-type strain, whereas development of the KO strain was terminated when initials of acervuli (arrow) had formed. Samples were stained with acid fuchsin. Bars = 10 μm.

(D) Relative DNA amounts of the *GPD1* gene from wild-type and KO strains in wounded and nonwounded leaves as determined by quantitative PCR at five time points. Letters indicate significance groups, and bars indicate ± SD (n = 3).

(E) Number of conidia produced by wild-type and KO strains on wounded and nonwounded leaves at 6 DAI. Patterns of columns are as in **(D)**. Bars indicate ± SD (n = 80, $P < 0.05$).

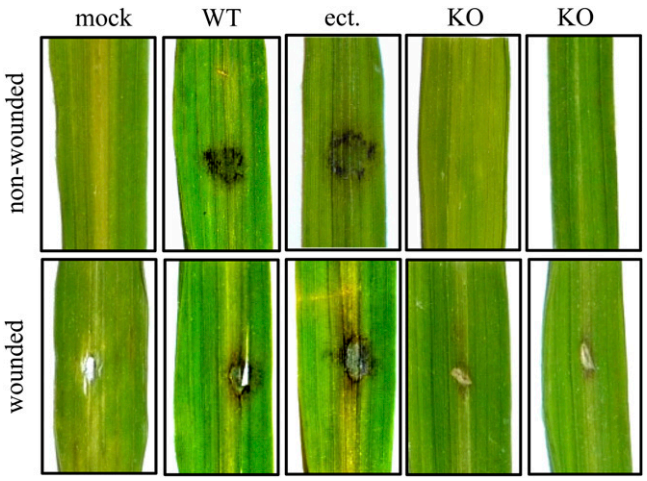

Figure 8. *Δppt1* Strains of *M. oryzae* Are Nonpathogenic on Rice.

Plant infection assays showed that the wild-type strain and a strain with an ectopic integration of the KO construct (ect.) infected and caused symptoms on wounded and nonwounded leaves 7 DAI. The *ΔMoppt1* (KO) strains were unable to cause disease symptoms on wounded or on nonwounded leaves. Representative photographs are shown. Three independent experiments were performed.

an ectopically integrated KO vector (Figure 8, ect.) were subsequently used in infection assays with intact and wounded leaves of the susceptible rice cultivar CO 39. As observed in infection assays with *Δppt1* strains of *C. graminicola* on maize, none of the *Δppt1* strains of *M. oryzae* were able to cause rice blast disease symptoms on wounded or on nonwounded leaves. By contrast, the wild-type strain and the strains carrying the ectopically integrated KO vector were able to cause disease symptoms in both wounded and nonwounded leaves (Figure 8).

Thus, infection assays performed with PPTase-deficient mutants of *C. graminicola* (Figure 7) and *M. oryzae* (Figure 8) suggest that PPTase is a fungal pathogenicity factor.

Enzymes Activated by PPT1 Are Required at Specific Stages of Pathogenesis

To investigate in more detail the pleiotropic phenotype of the PPTase-deficient mutant of *C. graminicola*, we compared the *Δppt1* strains with the melanin-deficient mutant M1.502 (Rasmussen and Hanau, 1989) and a Lys-auxotrophic mutant lacking the AAR gene (*Δaar1*) (Figure 9).

As described previously (Rasmussen and Hanau, 1989), the UV-induced mutant M1.502 was unable to cause disease symptoms when inoculated onto nonwounded maize leaves (Figure 9A), due to its inability to differentiate melanized appressoria (Figure 9B, M1.502). Even 32 HAI, the nonmelanized appressoria (note aniline blue–stained hyaline appressoria on the cuticle) had not penetrated the cuticle. Several of these nonmelanized appressoria had either germinated laterally (Figure 9B, 32 HAI, left micrograph, arrows) or ruptured (Figure 9B, 32 HAI, right micrograph, arrow). Cell wall rupturing had also been observed with the nonmelanized appressoria of *Δppt1* strains (Figures 5D and 5E). Disruption of appressorial cell walls in nonmelanized strains due to misregulated turgor pressure is unlikely, as cytorrhizis experiments with increasing concentrations of polyethylene glycol 6000 showed that the turgor pressure of appressoria of strain M1.502 was comparable to that of the wild-type strain (see Supplemental Figure 8 online). General defects in cell wall integrity, as indicated by hyphal swellings, were not observed in saprophytically growing or in pathogenic hyphae developing in wounded leaves. Hyphae of strains *Δppt1* and M1.502 exhibited normal cell walls even at apical regions and were able to penetrate anticlinal cell walls of plant cells (Figure 7C, 2 DAI, arrows; Figure 9C, 72 HAI, arrow) after inoculation onto wounded leaves. On wounded leaves, strain M1.502, but not the *Δppt1* strains, was able to cause spreading anthracnose disease symptoms (Figures 7B and 9A). These data suggest that melanization catalyzed by a 4'-PPTase-dependent PKS contributes to the appressorial cell wall stability specifically required in infection cells generating high turgor pressure.

As expected, the nonmelanized strain M1.502 was able to form acervuli and conidia normally (Figure 9C, 120 HAI, arrow). Like appressoria, setae were nonmelanized in this strain (Figure 9B, 120 HAI, arrowhead).

To assess the role of AAR activity and Lys biosynthesis in pathogenesis, an AAR-deficient mutant of *C. graminicola* was created by deletion of the AAR-encoding gene *AAR1*. As described for deletion of the *PPT1* gene of *M. oryzae*, a KO construct consisting of the *hph* cassette flanked by ~1 kb of 5′- and 3′-flanks of the *AAR1* gene (see Supplemental Figure 9 online) was transformed into protoplasts of the WT strain CgM2 of *C. graminicola*. Homologous integration of the KO fragment was confirmed by DNA gel blot analysis (see Supplemental Figure 9 online).

Infection assays were performed on wounded and nonwounded leaf segments with the wild-type strain, transformants carrying an ectopically integrated KO construct, and two independent *Δaar1* strains (Figure 9). In contrast with the wild-type strain and the ectopic strain (Figure 9A, WT and ect.), the *Δaar1* strains (Figure 9A, *Δaar1*, KO) were unable to cause disease symptoms on nonwounded leaves. Microscopy analyses showed that both independent *Δaar1* strains used in these assays formed melanized appressoria on the cuticle and were able to penetrate intact maize leaves (Figure 8B, *Δaar1*, 32 HAI, left micrograph), although penetration rates were reduced (32.7% ± 2.1% and 26.0% ± 4.5% penetration in two independent transformants compared with 69.3% ± 4.5% in the wild-type strains at 32 HAI). Reduced penetration rates are likely not due to reduced turgor pressure in appressoria of *Δaar1* strains, as indicated by cytorrhizis experiments (see Supplemental Figure 8 online).

Surprisingly, *Δaar1* strains were only able to differentiate biotrophic infection structures (i.e., infection vesicles and young primary hyphae) (Figure 9B, *Δaar1*, 32 HAI, –lys, arrows) and failed to form necrotrophic secondary hyphae, possibly due to Lys starvation. Supporting this assumption, when 0.34 mM Lys was added to the infection droplet (Figure 9B, *Δaar1*, 32 HAI, + lys, arrows) or when conidia were inoculated onto wounded leaves, necrotrophic secondary hyphae formed (Figure 9B, *Δaar1*, 72 HAI, arrow) and caused anthracnose disease

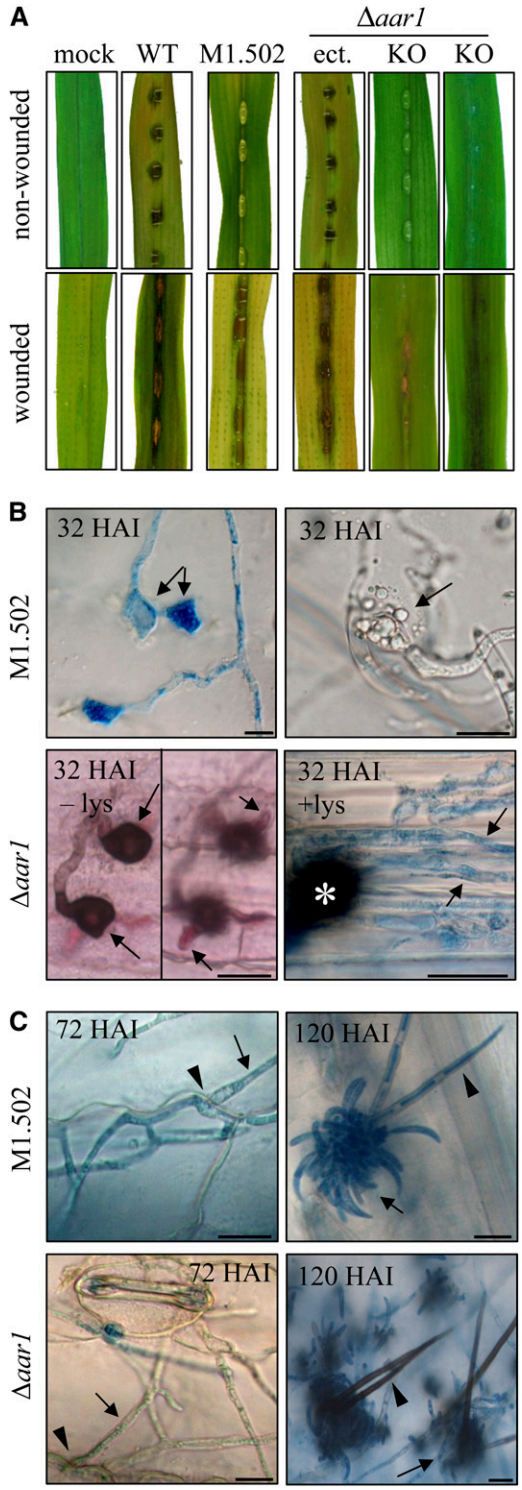

Figure 9. Synthesis of Melanin and Lys Is Required for Pathogenicity.

(A) Plant infection assays showed that the wild type, but not the melanin-deficient strain M1.502 or the Lys-deficient Δ*aar1* strain (KO), caused anthracnose disease symptoms on nonwounded maize leaves. Symptom development was restored on wounded leaves; a strain with an ectopic integration of the *AAR1* KO construct and mock-inoculated leaves served as controls.

(B) Micrographs of intact leaves inoculated with M1.502 showed functionally aberrant appressoria on the intact plant surface, as indicated by lateral germination (32 HAI, left image, arrows) or ruptured appressoria (32 HAI, right image, arrow). Δ*aar1* strains formed melanized appressoria (32 HAI, – lys, left image, arrows) and primary infection hyphae (32 HAI, – lys, right image, arrows), which were unable to form secondary hyphae and to switch to necrotrophic development. Addition of Lys restored the ability to switch to necrotrophy, as indicated by the occurrence of thin intracellular secondary hyphae (32 HAI, + lys, arrows; asterisk marks appressorium). All samples, except Δ*aar1*, 32 HAI, – lys, which was acid fuchsin-stained, were aniline blue stained. Bars = 10 μm.

(C) On wounded leaves, M1.502 and Δ*aar1* strains formed secondary hyphae (72 HAI, arrows) penetrating anticlinal cell walls (72 HAI, arrowhead). Asexual sporulation occurred in both strains (120 HAI, arrows). In contrast with melanized setae of strain Δ*aar1* (120 HAI, arrowhead), setae of strain M1.502 were nonmelanized (120 HAI, arrowhead). Samples were stained with aniline blue. Bars = 10 μm.

symptoms (Figure 9A, *AAR1*, KO wounded). Δ*aar1* strains were delayed in sporulation, but by 120 HAI, acervuli with melanized setae (Figure 9C, Δ*aar1*, 120 HAI, arrowhead) and normal spores (Figure 9C, Δ*aar1*, 120 HAI, arrow) had formed on infected leaves.

In summary, melanization is required at the stage of appressorium formation, and AAR activity is needed to enter necrotrophic development. The Sfp-type PPTase PPT1 of *C. graminicola* activates AAR, PKSs, and NRPSs and is required for conidiation, infection-related morphogenesis, appressorium function, and anthracnose disease development. Furthermore, our data show that PPTase activity is indispensable for pathogenicity in two different fungi and very likely in other filamentous pathogenic fungi.

DISCUSSION

In crop plants, fungi cause more economic damage than any other group of microorganisms, with annual losses estimated at more than $200 billion (Birren et al., 2002). Reduction of yield, however, represents only part of problems associated with fungal plant pathogens. *Aspergillus* and *Fusarium* species, and others, produce highly toxic secondary metabolites called mycotoxins, and uptake of contaminated food may result in increased incidence of cancer (Desjardins et al., 2000). Furthermore, several secondary metabolites (e.g., various toxins, melanin, and siderophores) represent pathogenicity factors in fungi attacking plants and mammals (Howard et al., 1991; Langfelder et al., 2003; Baker et al., 2006; Oide et al., 2006; Haas et al., 2008). Therefore, understanding fungal secondary metabolism at the molecular level may allow developing novel strategies to combat fungal diseases in both agriculture and medicine.

The use of drugs interfering with the formation of single secondary metabolites may have a limited application range, as many of these only play a role in some fungi. Melanin biosynthesis inhibitors, for example, are specifically used in rice blast control (Sawada et al., 2004), but other economically important plant pathogens, such as rusts and powdery mildews, are not affected as they are nonmelanized. By contrast,

PPTases, which simultaneously activate AAR, type I and II PKSs, NRPSs, and NRPS/PKS hybrids, could represent novel targets for drugs and alternative antifungal strategies to efficiently combat a broad range of pathogens infecting either mammals or plants. In addition to blocking synthesis of PKs, NRPs, and NRP/PK hybrid molecules, interference with AAR activity may increase drug efficiency and specificity, as only in fungi does Lys biosynthesis occur via AAR. Indeed, deletion of the *A. fumigatus* Lys biosynthesis gene *lysF* encoding homoaconitase led to attenuated virulence in a low-dose mouse infection model of invasive aspergillosis (Liebmann et al., 2004).

Infection assays with PPTase-deficient mutants of *C. graminicola* revealed that *PPT1* is required for differentiation of functional melanized appressoria and penetration competence, anthracnose disease symptom formation, and asexual sporulation. Surprisingly, however, when inoculated onto wounded leaves *Δppt1* mutants were able to invade and spread within the host tissue. These observations suggest that in *Δppt1* strains, which are unable to activate NRPSs and AAR, additional components may guarantee supply with iron and Lys during in planta growth. For example, a high affinity iron uptake system (Eichhorn et al., 2006) may compensate for the lack of siderophores and uptake of free Lys, which is present at a concentration of ~0.1 mM in maize cells (Chapman and Leech, 1979), may compensate for Lys auxotrophy. Alternatively, Lys may be provided by protein degradation by secreted proteases (Krijger et al., 2008). Interestingly, PPTase-deficient mutants are able to ramify within the host tissue but are unable to cause anthracnose disease symptoms, suggesting that toxins formed by PKSs, NRPSs, or PKS/NRPS hybrids might be required for a necrotrophic lifestyle.

To further investigate the different roles played by the enzymes and metabolic pathways activated by PPT1, a melanin-deficient mutant strain, M1.502 (Rasmussen and Hanau, 1989), and AAR-deficient mutants produced in this work were analyzed for defects in pathogenesis. Strain M1.502 formed nonmelanized appressoria and was nonpathogenic on an intact plant surface but produced normal anthracnose disease symptoms on wounded leaves, confirming previous reports on melanin-deficient mutants of this and other plant pathogenic fungi (Rasmussen and Hanau, 1989; Tsuji et al., 2000; Wilson and Talbot, 2009). Interestingly, our study showed that nonmelanized appressoria of strain M1.502 (frequently) ruptured on the plant surface, as did the rarely formed appressoria of *Δppt1* strains, suggesting that melanization contributes to cell wall rigidity, which counteracts the enormous turgor pressure (5.35 MPa) generated in these infection cells (Bechinger et al., 1999). Although it is widely accepted that in the appressorial cell walls of the rice blast fungus *M. oryzae* melanin acts as a barrier to the efflux of osmolytes and is needed for turgor generation (Howard and Ferrari, 1989; Wilson and Talbot, 2009), studies with *Gaeumannomyces graminis* var *graminis* have shown that melanization is also associated with cell wall rigidity (Money et al., 1998). Other causes for appressorial rupture in *Δppt1* strains and in strain M1.502 of *C. graminicola* (e.g., the occurrence of general cell wall or cytoskeleton defects) (Kopecká and Gabriel, 1995; Scheffer et al., 2005; Takeshita et al., 2006; Werner et al., 2007) are unlikely, as hyphae of these strains growing in vitro or in planta showed no apical or subapical swellings. In addition, cytorrhizis experiments revealed that no significant differences in appressorial turgor exist between the wild type and strain M1.502. Thus, melanization of appressoria is the first step requiring PPT1 activity in the infection process and is mediated by activating a PKS (Figure 10). In *C. graminicola*, the PKS required for melanization of appressoria likely is PKS1, as the gene encoding this enzyme is specifically activated during appressorium differentiation (Sugui and Deising, 2002).

To assess the role of AAR1 and Lys biosynthesis in infection structure formation and pathogenesis, we deleted the *AAR1* gene of *C. graminicola*. Δ*aar1* strains differentiated melanized appressoria but showed significantly reduced penetration rates. Again, cytorrhizis experiments showed that turgor pressure of appressoria of wild-type and Δ*aar1* strains were similar. Interestingly, appressoria of *Δaar1* strains that were able to penetrate the epidermal cell of their host plants formed biotrophic structures (i.e., infection vesicles and primary hyphae) but failed to form secondary hyphae and to switch to necrotrophic development (Figures 9B and 10). Addition of Lys to the infection droplet complemented this defect (Figure 9B), suggesting that the apoplasmic Lys concentration in maize leaves is too low to support growth of primary hyphae and to switch to necrotrophy. In agreement with this hypothesis, when *Δaar1* strains were inoculated onto wounded leaves that were releasing cytoplasm containing amino acids and proteins, necrotrophic secondary hyphae formed and gave rise to typical disease symptoms.

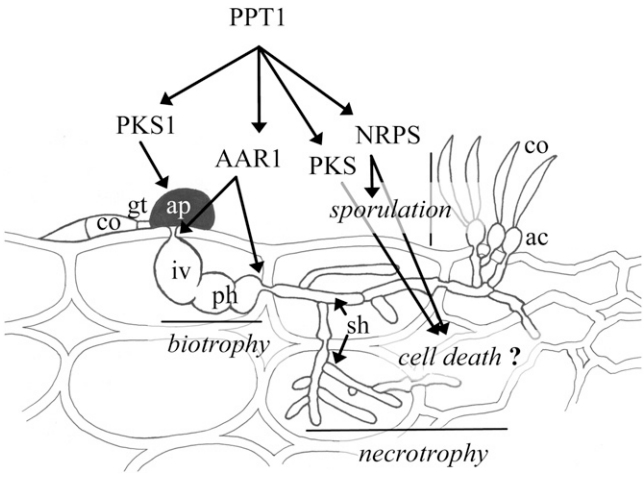

Figure 10. 4'-Phosphopantetheinyl Transferase (PPT1) Is a Central Regulator of Pathogenicity of *C. graminicola*.

All PKSs, NRPSs, and AAR1 require activation by PPT1. Appressoria of melanin-deficient mutants are unable to invade the host, and AAR-deficient mutants show reduced penetration competence and form biotrophic infection structures but are unable to switch to a necrotrophic lifestyle. PPT1-deficient mutants are unable to kill the host cells, possibly due to their inability to synthesize toxic PKS- and/or NRPS-dependent secondary metabolites. PPT1-deficient mutants are also unable to sporulate, probably due to their inability to synthesize siderophores by NRPSs. ac, acervulus; ap, appressorium; co, conidium; gt, germ tube; iv, infection vesicle; ph, primary hypha; sh, secondary hypha. Artwork not to scale.

However, if *C. graminicola* should produce ribosomal peptide toxins as reported for the barley (*Hordeum vulgare*) and rye (*Secale cereal*) pathogen *Rhynchosporium secalis* (NipA) (Rohe et al., 1995) and the wheat (*Triticum aestivum*) pathogen *Pyrenophora tritici repentis* (ToxA) (Manning et al., 2007), one may consider that Lys could indirectly be required for toxin synthesis and entering of the necrotrophic lifestyle.

Comparative analyses of culture filtrates of *C. graminicola* wild-type and *Δppt1* strains allowed us to identify several as yet unknown secondary metabolites (Figure 3). As *Δppt1* strains were unable to kill host cells and to cause disease symptoms, we hypothesized that the compounds identified may act as toxins. Some of the secondary metabolites only formed by the wild-type strain; for example, orcinol, indole-3-ylacetic acid, tryptophol, colletopyrones B and C, colletoanthrone A, himanimide C, colletoquinones A and B, and colletolactone A were present in culture filtrates at concentrations allowing purifying them. However, when applied onto wounded and nonwounded maize leaves, toxic effects were not observed. This also held true when a combination of all compounds was tested. However, toxins affecting the host tissue during the infection process may not be synthesized during saprophytic growth in liquid media. Analysis of spore germination fluids of the fungus *C. carbonum* by plasma desorption mass spectrometry showed that synthesis and release of the host-selective HC toxin, a member of the NRP class of toxins, was coincident with maturation of appressoria. Spores incubated under conditions that did not induce appressorium formation failed to produce the toxin, indicating that toxin synthesis is regulated by infection-related morphogenesis (Weiergang et al., 1996). Future studies employing thin membranes that allow forceful penetration and formation of infection structures comparable to those normally formed in planta (Küster et al., 2008) may help identify PK or NRP toxins exclusively formed by specific infection structures.

The ability to sporulate is essential for completion of the disease cycle of *C. graminicola*. *Δppt1* strains were unable to sporulate on infected plant tissue (Figure 6). A conditional *cfwA2* mutation in *A. nidulans* enhanced the sporulation defects of both *ΔtmpA* and *ΔfluG* single mutants, suggesting that unidentified CfwA-dependent PKSs and/or NRPSs are involved in the production of unknown compounds required for sporulation (Soid-Raggi et al., 2006; Marquez-Fernandez et al., 2007). However, delayed sporulation has been observed in *Δaar1* strains, and mutants of *C. graminicola* that are unable to synthesize siderophores are unable to sporulate (E. Albarouki and H.B. Deising, unpublished data). Sporulation defects in *Δppt1* strains may therefore be due to various reasons, such as insufficient supply of Lys or iron in the host tissue and lack of PKS-, NRPS-, or PKS/NRPS-hybrid-dependent secondary metabolites serving as a sporulation signal.

Our analyses have shown that PPT1 affects pathogenicity of *C. graminicola* at different morphogenetic stages through activating enzymes of primary (AAR1) and secondary (PKS1 and possibly other PKSs and NRPSs) metabolism (Figure 10). Although this work has not identified PPT1-dependent toxic secondary metabolites, our data highlight the central role played by PPT1 in switching to destructive necrotrophic disease development.

Our findings contribute to the understanding of fungal pathogenicity. The novel fungal pathogenicity factor identified (i.e., PPTase) is not only of scientific interest but could also be applied to screen for novel lead structures in medical or agricultural pharmacology or in biotechnology. Furthermore, PPTases may also represent a promising target in novel host-induced gene silencing strategies. These RNA interference (RNAi)-based disease control strategies have recently been discovered by Schweizer et al. (2006). These authors have shown that expression of RNAi constructs targeting genes essential for pathogenic development of the powdery mildew fungus *Blumeria graminis* f. sp *hordei* and the *Fusarium* head blight fungus *G. zeae* in barley drastically reduced disease development (Schweizer et al., 2006; Gay et al., 2008). RNAi-mediated silencing of PPTase genes by either expressing RNAi constructs corresponding to conserved PPTase domains or by expressing multiple constructs corresponding to individual PPTase genes of different fungi may improve resistance to several pathogens simultaneously.

METHODS

Fungal Isolates, Culture Conditions, and Infection Assays

The wild-type strain CgM2 of *Colletotrichum graminicola* (Cesati) Wilson (teleomorph *Glomerella graminicola* [Politis]) was provided by R.L. Nicholson, Purdue University, IN.

Synthetic minimal medium contained 1% (w/v) glucose, 1 g/L Ca $(NO_3)_2$, 0.2 g/L KH_2PO_3, 0.25 g/L $MgSO_4$, 0.054 g/L NaCl, and 1.5% (w/v) agarose with or without 50 μg/ml L-Lys. Synthetic complete medium [1.7 g/L yeast nitrogen base without amino acids (Becton Dickinson), 5 g/L $(NH_4)_2SO_4$, 20 g/L glucose, and amino acid mixture (Treco and Lundblad, 1993)] was supplemented with 100 μM bathophenanthroline-disulfonate (Sigma-Aldrich), with or without 50 μM desferri-coprogen (EMC Microcollections) or desferri-ferrichrome (Sigma-Aldrich).

Sensitivity to reactive oxygen species was determined on potato dextrose agar (Becton Dickinson) supplemented with 0.0075% (v/v) H_2O_2 (Carl Roth) in darkness or with 100 μg/ml rose bengal under constant light (10 μE) at 23°C.

Infection structures were induced as described (Werner et al., 2007). *Magnaporthe oryzae* strain 70-15 (Fungal Genetics Stock Center) was cultured as described (Hof et al., 2007). PPTase-deficient mutants of *C. graminicola* and *M. oryzae* were grown in media supplemented with 50 mg L-Lys/L.

Saccharomyces cerevisiae Δ*lys5* mutant BO4421 (Mat a, his3Δ1, leu2Δ0, met15Δ0, ura3Δ0, YGL154c:kanMX4) and the reference strain BY4741 (Mat a, his3Δ1, leu2Δ0, met15Δ0, ura3Δ0) (Euroscarf) were grown at 30°C and 150 rpm in liquid YPD complete or SD minimal medium or on corresponding solidified media (Sambrook et al., 1989). BO4421 was grown in the presence of 50 mg L-Lys/L.

Fourteen-day-old whole maize (*Zea maize* cv Nathan) plants, leaf segments (1st to 3rd leaf, depending on the experiment) or epidermal cell layers from onion bulbs (*Allium cepa* cv Grano) were used to assess virulence of CgM2 and transformants. Inoculation was performed with 10-μL droplets containing 10^3 conidia in 0.01% (v/v) Tween 20. To inoculate wounded leaves, single pricks (DB Micro-Fine, 0.2 mm 33G Sterile Lancets; Becton Dickinson) were inserted immediately prior to inoculation. Leaf segments (8 cm) were incubated in sealed Petri dishes in a BOD 400 incubator (Uni Equip) in darkness at 23°C. Symptoms were photographed 6 DAI. Alternatively, 0.5 g mycelium of 10-d-old liquid CM cultures was washed with distilled water twice and fragmented in 15 mL sterile 0.01% (v/v) Tween 20 using an Ultra Turrax (IKA Labortechnik).

Maize plants were sprayed with mycelial fragment suspensions. Mock inoculation was performed using sterile 0.01% (v/v) Tween 20. Plants were incubated in a Percival AR-75L growth chamber (12 h light; 200 μE; 70% relative humidity; 25°C). Anthracnose lesions were photographed 6 DAI.

To quantify conidiation, 10 infected leaf segments of each category were washed vigorously 6 DAI in 2 mL 0.01% (v/v) Tween 20, and conidia were counted in a Thoma chamber.

Rice plants (*Oryza sativa* cv CO-39) were grown as described (Hof et al., 2007). Detached leaf assays were performed with 10- to 15-cm-long segments of leaves from 21-d-old rice plants. Wounded and nonwounded leaf fragments were inoculated with washed mycelial plugs and incubated in sealed Petri dishes under rice growth conditions for 7 d.

All experiments were performed in triplicate.

Extraction of RNA and Construction of a *C. graminicola* cDNA Expression Library in Yeast

Total RNA was extracted from melanized mycelium (Chirgwin et al., 1979); mRNA was isolated using the Nucleotrap mRNA Purification Kit (BD Biosciences Clontech), and cDNA synthesis was performed using the Creator SMART cDNA Library Construction Kit (Clontech).

The yeast cDNA expression vector pAG300 (www.addgene.org) was constructed by inserting a *Sfi*I cassette into the *Hin*dIII + *Xho*I digested plasmid pVT102U (Vernet et al., 1987). The *Sfi*IA and *Sfi*IB sites allowed unidirectional cloning of the cDNA library. The *C. graminicola* cDNA library, pcfwA (pAG300 containing the *cfwA* cDNA of *Aspergillus nidulans*), or empty vector (pAG300) were transformed into *S. cerevisiae* strain BO4421 using the lithium acetate procedure (Becker and Lundblad, 2001). Cells were grown on synthetic dextrose agar lacking uracil and Lys.

Targeted Inactivation of *PPT1* and *AAR1* of *C. graminicola* and of *PPT1* of *M. oryzae* and Complementation of *C. graminicola* Δ*ppt1* Strains

The complete genomic *PPT1* sequence of *C. graminicola*, including 1232 bp of the 5′-region, was obtained by genome walking (Liu and Baird, 2001).

The *Eco81*I-*hph* cassette from pUC ATPH SI (Lu et al., 1994) was used to replace the 182-bp *Eco81*I fragment of *C. graminicola PPT1*. The resulting 4710-bp *PPT1* knockout (KO) construct had 1430-bp 5′ and 709-bp 3′ homologous regions flanking the *hph* gene. Transformation of the KO construct into conidial protoplasts was done as described (Werner et al., 2007).

The 3.1-kb complementation vector consisted of 1232 bp of the *PPT1* promoter region, the complete coding region, and the *trpC* terminator of *A. nidulans*. Transformants were plated out on selection medium [1 M sucrose, 1.7 g/L yeast nitrogen base without amino acids (Becton Dickinson), 5 g/L $(NH_4)_2SO_4$, and 1.5% (w/v) agarose] that did not allow growth of Lys auxotrophs.

The *AAR* KO construct was assembled by double-joint-PCR (Yu et al., 2004). First, flanking regions were amplified with primers CgAARKO5′1, 5′-AAAGGGTGTTCGGTCCTCTAC-3′, and CgAARKO5′2, 5′-GATTCTATAGGAAGATCCAGGCACCGGTCATTGATCGTAGGTGCTCCGAAC-3′, and primers CgAARKO3′1, 5′-GAGGGCAAAGGAATAGAGTAGATGCCGACCTGGCGCTTTGGTCTAAGTAAC-3′, and CgAAR KO3′2, CTCCGAGACCTAGGCTAGTAAAG-3′ (sequence overlaps with the *hph* cassette are underlined). The *hph* cassette from vector pAN7-1 was amplified with primers hph1, 5′-TGACCGGTGCCTGGATCTTCCTATAGAATC-3′, and hph2, 5′-GGTCGGCATCTACTCTATTCCTTTGCCCTC-3′. In a second PCR, the products of the first step amplified in separate reactions were fused, and the complete product was amplified using nested primers CgAARKOnes1 (5′-CCATCCGTGTGGAGGAGTTG-3′) and CgAARKOnes2 (5′-AGGGAGAGGGCATACTTGACTG-3′). Transformation of the KO construct into conidial protoplasts was done as described (Werner et al., 2007).

To delete the *PPT1* gene of *M. oryzae*, a 3135-bp DNA fragment, including the *PPT1* open reading frame and ~1000 bp upstream and downstream flanking regions, was amplified by PCR using primers MoPPT1KO1 (5′-CCCCAATACGTAGCACTA-3′) and MoPPT1KO2 (5′-GTGTTACGGATAAAACGACCG-3′) and cloned into pGEM-T Easy (Promega). An 870-bp fragment (−60 bp to 810 bp relative to ATG) was released by restriction digestion with *Eco81*I/*Stu*I and replaced by the 2.6-kb *hph* cassette from vector pAN7-1 (Punt et al., 1987). The complete KO construct was released by *Not*I digestion and cloned into the *PspOM*I site of vector pCAMBIA0380 (GenBank accession number AF234290.1).

Agrobacterium tumefaciens–mediated transformation was performed essentially as described (Hof et al., 2007). Media were supplemented with 50 mg L-Lys/L to allow growth of Lys auxotrophs.

Expression of the *PPT1*:*eGFP* Fusion Construct in *C. graminicola*

The DNA sequence upstream of *PPT1* was determined by genome walking (Liu and Baird, 2001).

A PCR with primers EGFP1 (5′-TTACCGGTTTGTTGGGGTCTCAAAAGGATG-3′; *Age*I site underlined) and EGFP2 (5′-TTTTCGAAACTTTGATGACTCTCCCCAA-3′; *Bsp 119*I site underlined) yielded a 2329-bp fragment containing the *PPT1* open reading frame and 1.2 kb of the promoter region. Cloning into pGEM-T Easy (Promega) resulted in plasmid pPPTfl. The unique *Bsp119*I site was then used to fuse a 1.5-kb PCR fragment containing the *eGFP* open reading frame and the *TrpC* terminator (primers EGFP3, 5′-TTTTCGAAATGGTGAGCAAGGGCGAG-3′, *Bsp119*I site underlined, and EGFP4, 5′-TTTTCGAACGCAGGACAATCGCTACAG-3′; *Bsp119*I site underlined) from vector pSH1.51EGFP in frame with *PPT1*. To introduce a resistance marker, the 2.4-kb *hph* cassette of pHPHAgeI (i.e., pCR2.1; Invitrogen), containing the *hph* gene flanked by *Age*I sites, was excised and cloned into the corresponding *Age*I site of the *eGFP* fusion vector.

The complete 5.94-kb *PPT1*:*eGFP* fusion construct was excised from pGEM-T Easy by *Not*I digestion, purified by gel elution, and transferred into conidial protoplasts as described (Werner et al., 2007).

DNA Extraction and Genomic DNA Gel Blot Analysis

Genomic DNA was isolated from 500 mg of vegetative mycelia of *C. graminicola*, following the method described (Döbbeling et al., 1997).

To perform genomic DNA gel blot analyses, 10 μg of *Pst*I-digested DNA was separated on a 0.8% (w/v) agarose gel in TAE buffer, depurinated, and blotted onto a positively charged nylon membrane (Hybond-N^+; Amersham Pharmacia Biotech) by downward alkaline capillary transfer (Brown, 1999). Specific primers CgPPT probe1 (5′-AACGTCTCAACCTCCCCC-3′), CgPPT probe2 (5′-ACGCTACAGGCAAGATCG-3′), and plasmid pPPTfl template DNA were used to generate a 511-bp alkalilabile DIG-dUTP–labeled probe (Roche Diagnostics).

To analyze transformants for the presence/absence of *C. graminicola AAR1*, 5 μg of *Eco81*I-digested genomic DNA was separated and blotted as described above. Specific primers Cg-SQ_7 (5′-ACAGCGGTCATTGACTGGAG-3′) and CgAAR-probe2-rev (5′-GTGGTGAGAGGTGCAGACAAG-3′) and the KO construct as PCR template were used to amplify a 1000-bp DIG-dUTP–labeled probe.

M. oryzae PPT1 deletions were identified using a specific 400-bp probe amplified from genomic DNA with primers MoPPT1 probe forward (5′-AGAGACTTGCAGGGACTCC-3′) and MoPPT1 probe reverse (5′-CTCTTCACCTCTGCATTCG-3′). Five micrograms of *Xho*I-digested genomic DNA per lane was used for DNA gel blot analysis.

Hybridization and probe detection followed the recommended protocol (Roche Diagnostics). The membrane was exposed to Hyperfilm ECL X-ray film (Amersham Pharmacia Biotech).

RT-PCR and Quantitative PCR

Gene-specific primers used to analyze expression of the *PPT1* gene were PPTORF1 (5′-ATGGCCCCGACTATCATACAGTGG-3′) and PPTORF2 (5′-CTAACTTTGATGACTCTCCCCAAAAG-3′). Primers for the constitutively expressed chitin synthase gene *CHSII* were CHSII1 and CHSII3 (Werner et al., 2007). One-hundred nanograms of total RNA (for *PPT1*) or 50 ng (for *CHSII*) pretreated with RQ1 RNase-free DNase (Promega) were used in 10-μL RT-PCR reactions (One Step RT-PCR Kit; Qiagen). cDNA synthesis was performed at 50°C for 30 min. Cycling conditions consisted of an initial denaturation step (95°C, 3 min), followed by 40 cycles of denaturation (95°C, 30 s), annealing (60°C, 20 s), and extension (72°C, 50 s).

Quantitative PCR was performed using a MyiQ-Single Color Real-Time PCR Detection System (Bio-Rad Laboratories) equipped with iQ5 standard edition software (version 2.0.148.60623). DNA was isolated as described above with an additional phenol-chloroform extraction and precipitated (SureClean solution; Bioline).

Reactions contained 100 ng template DNA, 100 nM of each primer (CgGPD-q1, 5′-TGAACGCGAGCTAACTTGACA-3′; CgGPD-q2, 5′-GGGCATCGAAGATGGAGGA-3′), and 10 μL iQ SYBR Green Supermix (Bio-Rad Laboratories) in a final volume of 20 μL. Cycling conditions consisted of an initial denaturation (95°C, 3 min), followed by 40 cycles of denaturation (95°C, 30 s), annealing (63°C, 20 s), and extension (72°C, 15 s). Melting curve and agarose gel analyses indicated amplification of a single product. PCR efficiency was calculated using the LinRegPCR software version 7.2 (Ramakers et al., 2003). C_T values of three independent replicates were used to calculate average values and standard deviations. All values are standardized to the average threshold cycle value obtained with DNA extracted from nonwounded leaves inoculated with the *C. graminicola* wild-type strain at 0 HAI.

α-Aminoadipate Reductase Activity (EC 1.2.1.31)

Yeast strains (BY4741, the Δ*lys5* mutant strain BO4421, and BO4421 transformants TcfwA, TAG2, TAG5, and TpAG300) were grown in YPD medium to the logarithmic growth phase (2×10^7 cells/mL), harvested by centrifugation (5 min, 5000*g*, 4°C), resuspended in 250 μL 75 mM Tris-HCl buffer, pH 8.0, and disrupted in 2.0-mL reaction tubes (Eppendorf) containing glass beads (425 to 600 μm; Sigma-Aldrich) by vortexing at 4°C for 10 min. After centrifugation (20,500*g*, 10 min, 4°C), supernatants were used to determine α-aminoadipate reductase activity by spectrophotometry at a wavelength of 340 nm. Reaction mixtures contained 75 mM Tris-HCl, pH 8.0, 2.5 mM DTT, 10 mM $MgCl_2$, 10 mM L-α-aminoadipate, 10 mM ATP, 0.4 mM NADPH, and 1 mg crude protein extract/mL. Consumption of NADPH was used to quantify enzyme activity. Assays were performed at 30°C. Degradation of NADPH in the absence of α-aminoadipate served as reference.

Protein concentrations were determined with the Bio-Rad protein assay and γ-globulin as standard.

Purification of $(His)_6$-PPT1 and the PKS100 Fragment and the 4′-Phosphopantetheinylation Assay

The *C. graminicola PPT1* cDNA was cloned into the *Nde*I-*Not*I–digested expression vector pET28a (Novagen). A 300-bp PCR fragment (nucleotides 4969 to 5268) of *PKS1* (Sugui and Deising, 2002) covering one 4′-phosphopantetheinylation site was cloned into the *Eco*RI- and *Not*I-digested vector pGEX-4T-1 (GE Healthcare). The plasmids were transformed into *Escherichia coli* BL21 DE3 (Studier and Moffatt, 1986), and expression of recombinant proteins and cell lysis were performed as described (Smith and Corcoran, 1994). PPT1 and PKS1 were N-terminally fused to a $(His)_6$ tag and GST, respectively, separated by a thrombin cleavage site.

Proteins were purified using the ÄKTAprime system (GE Healthcare) at 4°C. The cleared cell lysate containing $(His)_6$-PPT1 was loaded onto a HiTrap DEAE FF column equilibrated with 20 mM Tris/HCl, pH 8.0, and 1 mM DTT. The flow-through was loaded onto a HisTrap FF column equilibrated with 20 mM HEPES/NaOH, pH 7.5, 500 mM NaCl, and 20 mM imidazole. The bound $(His)_6$-PPT1 was eluted with a linear gradient of 0 to 500 mM imidazole in the same buffer. The cell lysate containing GST-PKS100 was loaded onto a GSTrap HP column equilibrated with 20 mM HEPES/NaOH, pH 7.5, and 50 mM NaCl and eluted in the same buffer supplemented with 10 mM reduced L-glutathione (Sigma-Aldrich). Fractions containing the affinity-tagged proteins were pooled, concentrated (Amicon Ultra; Millipore), and subjected to gel filtration on a HiLoad 16/60 Superdex 75 pg column in 20 mM HEPES/NaOH, pH 7.5, 1 mM DTT, and 10 mM $MgCl_2$. Finally, $(His)_6$-PPT1 and GST-PKS100 were concentrated and stored at −80°C.

Protein 4′-phosphopantetheinylation reactions were performed with fluorophore-conjugated CoA-488 (Covalys) essentially as described (Yin et al., 2005). Labeling reactions were analyzed by SDS-PAGE. Fluorescence was detected using a FLA-3000 phosphor imager (Fujifilm).

For MALDI-TOF MS (Ultraflex II; Bruker Daltonics) analyses, gel slices were treated with iodoacetamide followed by a tryptic digest (Zhbanko et al., 2005).

Analysis of Fungal Metabolites

C. graminicola CgM2 was grown in HMG medium (10 g/L malt extract, 4 g/L yeast extract, and 10 g/L glucose) in a 20-liter fermenter (Biolafitte) at 22 to 24°C with agitation (130 rpm) and aeration (3 L/min). Fermentation was stopped after 5 d, when the medium had been depleted of glucose. The mycelium was separated from the culture fluid by filtration (200 × 200-mm Tiefenfilter; Pall). The culture fluid was extracted with ethyl acetate, yielding 1.8 g crude extract, which was loaded onto a column containing silica gel (Merck 60) and eluted with 100% cyclohexane followed by cyclohexane/ethylacetate (9:1, 3:1, and 1:1, v/v), followed by ethylacetate and ethylacetate/methanol (3:1 and 1:1, v/v).

Preparative HPLC (Nucleosil-7 C18; RP 18, 250 × 10 mm, 7 μm; Macherey-Nagel) with a MeCN gradient (10 to 90%) over 40 min and a flow of 20 mL/min yielded compounds 1 to 12 (Figure 3).

Extraction and analysis of siderophores were done as described (Antelo et al., 2006; Meister et al., 2007).

Spectroscopy Methods for Compound Identification

Optical rotations were measured with a Krüss P8000 polarimeter at 589 nm. UV and IR spectra were measured with a Perkin-Elmer Lambda-16 spectrophotometer and a Bruker IFS48 FTIR spectrometer, respectively. NMR spectra were recorded with a Bruker Avance II spectrometer (400 MHz); the chemical shifts were referenced to the residual solvent signal ($CDCl_3$: δ_H = 7.26 ppm, δ_C = 77.16 ppm, CD_3OD: δ_H = 3.31 ppm, δ_C = 49.00 ppm, DMSO-d_6 δ_H = 2.50 ppm, δ_C = 39.52 ppm, MeCN-d_3: δ_H = 1.94 ppm). APCIMS spectra were measured with a Hewlett Packard MSD1100 instrument. ESI-HRMS spectra were recorded on a Micro-Mass/Waters ESI Q-TOF mass spectrometer equipped with a LockSpray interface using NaI/CsI or trialkylamines as external reference. FAB-HRMS spectra were measured with a VG70S (Xe-FAB ionization) using *m*-nitrobenzyl alcohol or glycerol as matrix and PEG 300 or 600 as the reference.

Microscopy

Fluorescence microscopy was performed on a Nikon Eclipse 90i confocal laser scanning microscope (Nikon) with the following settings: excitation wavelength, 488 nm; laser light transmittance, 25% (ND4 in, ND8 out); pinhole diameter, 30 μm; lens, Plan Apo 60/1.4 oil lens.

Bright-field and interference contrast microscopy were performed with a Nikon Eclipse E600 microscope as described (Werner et al., 2007). Incipient cytorrhizis was performed with different concentrations of polyethylene glycol 6000 (PEG 6000) as described (Howard et al., 1991). Acid fuchsin and anilin blue staining were performed as described (de Neergaard, 1997). Digital images were taken with a Cyber-shot DSC-W35 camera (Sony). Image processing was done with Adobe Photoshop software.

Statistics

Calculations (*t* test, analysis of variance) were done with the software XLSTAT version 2009.4.02 (Addinsoft).

Accession Numbers

Sequence data from this article can be found in the GenBank/EMBL database under the following accession numbers: *Colletotrichum graminicola PPT1*, DQ028305; *C. graminicola PKS1*, FJ194435; and *C. graminicola AAR1*, FN547151. The yeast expression vector pAG300 has been deposited in the Addgene (www.addgene.org) collection (plasmid 19363).

Supplemental Data

The following materials are available in the online version of this article.

Supplemental Figure 1. Complementation of Growth of the *S. cerevisiae* Δ*lys5* Mutant by the PPTase Genes of *A. nidulans* or *C. graminicola*.

Supplemental Figure 2. Generation of *Δppt1* Strains of *C. graminicola* by Homologous Recombination.

Supplemental Figure 3. Complementation of Growth of the Δ*ppt1* Mutant of *C. graminicola* by the Siderophore Desferri-Ferrichrome.

Supplemental Figure 4. Detection of the Intracellular Storage Siderophore Ferricrocin in Hyphal Extracts of *C. graminicola*.

Supplemental Figure 5. Characteristics of Identified Compounds Produced by the Wild-Type Strain but Not by *Δppt1* Strains of *C. graminicola*.

Supplemental Figure 6. Complementation of the *Δppt1* Strains with the *PPT1* Gene under Control of the Native Promoter Fully Rescues Growth Defects on Minimal Medium Lacking Lys.

Supplemental Figure 7. Generation of *Δppt1* Strains of *M. oryzae* by Homologous Recombination.

Supplemental Figure 8. Determination of Appressorial Turgor Pressure by Incipient Cytorrhizis with PEG 6000.

Supplemental Figure 9. Generation of *Δaar1* Strains of *C. graminicola* by Homologous Recombination.

Supplemental Table 1. ^{1}H (400 MHz) and ^{13}C (101 MHz) NMR Data of Colletopyrone B (CD_3OD) and Colletopyrone C ($CDCl_3$).

Supplemental Table 2. ^{1}H (400 MHz) and ^{13}C (101 MHz) NMR Data of Colletoquinone A (DMSO-d_6 + 30% CD_3OD) and Colletoquinone B ($CDCl_3$).

Supplemental Table 3. ^{1}H (400 MHz) and ^{13}C (101 MHz) NMR Data of Colletoanthrone A (DMSO-d_6).

Supplemental Table 4. ^{1}H (400 MHz) and ^{13}C (101 MHz) NMR Data of Colletolactone A ($CDCl_3$).

Supplemental References.

ACKNOWLEDGMENTS

Financial support by Volkswagenstiftung in the frame of the partnership program to J.A. and H.B.D. (Grant I/79 487) and by the Excellence Initiative of the State of Saxony-Anhalt to H.B.D. is gratefully acknowledged. Grant C01-1713 form SAGARPA-CONACYT to J.A. is also acknowledged. We thank A. Beutel, D. Jany, E. Vollmer, J.L. Ramos, and O. Sánchez for excellent technical support, D. Deising for artwork (Figure 10), A. Meffert and A. Schierhorn for HPLC/MS and MALDI-TOF MS analyses, H. Kolshorn and V. Sinnwell for NMR spectroscopy, N. Hanold and S. Franke for high-resolution mass spectrometry, A. Schüffler for helpful advice on the isolation of metabolites, W. Kummer and A. Mickel for help with microscopy, and J.-J. Krijger, H. Anke and T. Anke for stimulating discussions and support.

Received November 3, 2008; revised August 27, 2009; accepted October 5, 2009; published October 30, 2009.

REFERENCES

Antelo, L., Hof, C., Welzel, K., Eisfeld, K., Sterner, O., and Anke, H. (2006). Siderophores produced by *Magnaporthe grisea* in the presence and absence of iron. Z. Naturforsch. C **61:** 461–464.

Baker, S.E., Kroken, S., Inderbitzin, P., Asvarak, T., Li, B.Y., Shi, L., Yoder, O.C., and Turgeon, B.G. (2006). Two polyketide synthase-encoding genes are required for biosynthesis of the polyketide virulence factor, T-toxin, by *Cochliobolus heterostrophus.* Mol. Plant Microbe Interact. **19:** 139–149.

Bechinger, C., Giebel, K.-F., Schnell, M., Leiderer, P., Deising, H.B., and Bastmeyer, M. (1999). Optical measurements of invasive forces exerted by appressoria of a plant pathogenic fungus. Science **285:** 1896–1899.

Becker, D.M., and Lundblad, V. (2001). Introduction of DNA into yeast cells. In Current Protocols in Molecular Biology, F.M. Ausubel, R. Brent, R.E. Kingston, D.D. Moore, J.G. Seidman, J.A. Smith, and K. Struhl, eds (New York: John Wiley & Sons), pp. 13.17.11–13.17.10.

Bergstrom, G.C., and Nicholson, R.L. (1999). The biology of corn anthracnose. Knowledge to exploit for improved management. Plant Dis. **83:** 596–608.

Birren, B., Fink, G., and Lander, E. (2002). Fungal Genome Initiative: White Paper Developed by the Fungal Research Community. (Cambridge, MA: Whitehead Institute Center for Genome Research).

Brown, T. (1999). Southern blotting. In Current Protocols in Molecular Biology, F.M. Ausubel, R. Brent, R.E. Kingston, D.D. Moore, J.G. Seidman, J.A. Smith, and K. Struhl, eds (New York: John Wiley & Sons), pp. 2.9.1–2.9.15.

Chapman, D.J., and Leech, R.M. (1979). Changes in pool sizes of free amino-acids and amines in leaves and plastids of *Zea mays* during leaf development. Plant Physiol. **63:** 567–572.

Chirgwin, J.M., Przybyla, A.E., MacDonald, R.J., and Rutter, W.J. (1979). Isolation of biologically active ribonucleic acid from sources enriched in ribonuclease. Biochemistry **18:** 5294–5299.

Collemare, J., Billard, A., Böhnert, H.U., and Lebrun, M.H. (2008).

Biosynthesis of secondary metabolites in the rice blast fungus *Magnaporthe grisea*: The role of hybrid PKS-NRPS in pathogenicity. Mycol. Res. **112:** 207–215.

Dean, R.A., et al. (2005). The genome sequence of the rice blast fungus *Magnaporthe grisea.* Nature **434:** 980–986.

Deising, H.B., Werner, S., and Wernitz, M. (2000). The role of fungal appressoria in plant infection. Microbes Infect. **2:** 1631–1641.

De Jong, J.C., McCormack, B.J., Smirnoff, N., and Talbot, N.J. (1997). Glycerol generates turgor in rice blast. Nature **389:** 244–245.

de Neergaard, E. (1997). Methods in Botanical Histopathology. (Copenhagen, Denmark: Kandrups Bogtrykkeri).

Desjardins, A.E., Manandhar, G., Plattner, R.D., Maragos, C.M., Shrestha, K., and McCormick, S.P. (2000). Occurrence of *Fusarium* species and mycotoxins in nepalese maize and wheat and the effect of traditional processing methods on mycotoxin levels. J. Agric. Food Chem. **48:** 1377–1383.

Döbbeling, U., Böni, R., Häffner, A., Dummer, R., and Burg, G. (1997). Method for simultaneous RNA and DNA isolation from biopsy material, culture cells, plants and bacteria. Biotechniques **22:** 88–90.

Ehmann, D.E., Gehring, A.M., and Walsh, C.T. (1999). Lysine biosynthesis in *Saccharomyces cerevisiae*: Mechanism of alpha-aminoadipate reductase (Lys2) involves posttranslational phosphopantetheinylation by Lys5. Biochemistry **38:** 6171–6177.

Eichhorn, H., Lessing, F., Winterberg, B., Schirawski, J., Kämper, J., Müller, P., and Kahmann, R. (2006). A ferroxidation/permeation iron uptake system is required for virulence in *Ustilago maydis.* Plant Cell **18:** 3332–3345.

Fichtlscherer, F., Wellein, C., Mittag, M., and Schweizer, E. (2000). A novel function of yeast fatty acid synthase. Subunit alpha is capable of self-pantetheinylation. Eur. J. Biochem. **267:** 2666–2671.

Fudal, I., Collemare, J., Böhnert, H.U., Melayah, D., and Lebrun, M.H. (2007). Expression of *Magnaporthe grisea* avirulence gene *ACE1* is connected to the initiation of appressorium-mediated penetration. Eukaryot. Cell **6:** 546–554.

Fuganti, C., Mendozza, M., Joulain, D., Minut, J., Pedrocchi-Fantoni, G., Piergianni, V., Servi, S., and Zucchi, G. (1996). Biogeneration and biodegradation of raspberry ketone in the fungus *Beauveria bassiana.* J. Agric. Food Chem. **44:** 3616–3617.

Gay, A., Zimmermann, G., Nowara, D., Kumlehn, J., Schweizer, P., and Hensel, G. (2008). Triple RNAi constructs for broad-range resistance against fungal leaf diseases. Book of Abstracts, 9th International Congress of Plant Pathology 2008, Torino, Italy. J. Plant Pathol. **90** (suppl.), 267–268.

Greenshields, D.L., Liu, G., Feng, J., Selvaraj, G., and Wei, Y. (2007). The siderophore biosynthetic gene *SID1*, but not the ferroxidase gene *FET3*, is required for full *Fusarium graminearum* virulence. Mol. Plant Pathol. **8:** 411–421.

Guzmán-de-Peña, D., Aguirre, J., and Ruiz-Herrera, J. (1998). Correlation between the regulation of sterigmatocystin biosynthesis and asexual and sexual sporulation in *Emericella nidulans.* Antonie Van Leeuwenhoek **73:** 199–205.

Haas, H., Eisendle, M., and Turgeon, B.G. (2008). Siderophores in fungal physiology and virulence. Annu. Rev. Phytopathol. **46:** 149–187.

Han, Y.-J., and Han, D.-M. (1993). Isolation and characterization of null pigment mutant in *Aspergillus nidulans.* Korean J. Genet. **15:** 1–10.

Henson, J.M., Butler, M.J., and Day, A.W. (1999). The dark side of the mycelium: Melanins of phytopathogenic fungi. Annu. Rev. Phytopathol. **37:** 447–471.

Hof, C., Eisfeld, K., Welzel, K., Antelo, L., Foster, A.J., and Anke, H. (2007). Ferricrocin synthesis in *Magnaporthe grisea* and its role in pathogenicity in rice. Mol. Plant Pathol. **8:** 163–172.

Howard, R.J., and Ferrari, M.A. (1989). Role of melanin in appressorium function. Exp. Mycol. **13:** 403–418.

Howard, R.J., Ferrari, M.A., Roach, D.H., and Money, N.P. (1991). Penetration of hard substances by a fungus employing enormous turgor pressures. Proc. Natl. Acad. Sci. USA **88:** 11281–11284.

Keszenman-Pereyra, D., Lawrence, S., Twfieg, M.E., Price, J., and Turner, G. (2003). The npgA/cfwA gene encodes a putative 4'-phosphopantetheinyl transferase which is essential for penicillin biosynthesis in *Aspergillus nidulans.* Curr. Genet. **43:** 186–190.

Kopecká, M., and Gabriel, M. (1995). Actin cortical cytoskeleton and cell wall synthesis in regenerating protoplasts of the *Saccharomyces cerevisiea* actin mutant DBY 1693. Microbiology **141:** 1289–1299.

Krijger, J.-J., Horbach, R., Behr, M., Schweizer, P., Deising, H.B., and Wirsel, S.G.R. (2008). The yeast signal sequence trap identifies secreted proteins of the hemibiotrophic corn pathogen *Colletotrichum graminicola.* Mol. Plant Microbe Interact. **21:** 1325–1336.

Kroken, S., Glass, N.L., Taylor, J.W., Yoder, O.C., and Turgeon, B.G. (2003). Phylogenomic analysis of type I polyketide synthase genes in pathogenic and saprobic ascomycetes. Proc. Natl. Acad. Sci. USA **100:** 15670–15675.

Küster, S., Ludwig, N., Willers, G., Hoffmann, J., Deising, H.B., and Kiesow, A. (2008). Thin PTFE-like membranes allow characterizing germination and mechanical penetration competence of pathogenic fungi. Acta Biomater. **4:** 1809–1818.

Langfelder, K., Streibel, M., Jahn, B., Haase, G., and Brakhage, A.A. (2003). Biosynthesis of fungal melanins and their importance for human pathogenic fungi. Fungal Genet. Biol. **38:** 143–158.

Lee, B.N., Kroken, S., Chou, D.Y., Robbertse, B., Yoder, O.C., and Turgeon, B.G. (2005). Functional analysis of all nonribosomal peptide synthetases in *Cochliobolus heterostrophus* reveals a factor, NPS6, involved in virulence and resistance to oxidative stress. Eukaryot. Cell **4:** 545–555.

Liebmann, B., Mühleisen, T.W., Müller, M., Hecht, M., Weidner, G., Braun, A., Brock, M., and Brakhage, A.A. (2004). Deletion of the *Aspergillus fumigatus* lysine biosynthesis gene *lysF* encoding homoaconitase leads to attenuated virulence in a low-dose mouse infection model of invasive aspergillosis. Arch. Microbiol. **181:** 378–383.

Liu, X., and Baird, W.V. (2001). Rapid amplification of genomic DNA ends by *Nla*III partial digestion and polynucleotide tailing. Plant Mol. Biol. Rep. **19:** 261–267.

Lu, S., Lyngholm, L., Yang, G., Bronson, C., Yoder, O.C., and Turgeon, B.G. (1994). Tagged mutations at the *Tox1* locus of *Cochliobolus heterostrophus* by restriction enzyme-mediated integration. Proc. Natl. Acad. Sci. USA **91:** 12649–12653.

Manning, V.A., Hardison, L.K., and Ciuffetti, L.M. (2007). Ptr ToxA interacts with a chloroplast-localized protein. Mol. Plant Microbe Interact. **20:** 168–177.

Marquez-Fernandez, O., Trigos, A., Ramos-Balderas, J.L., Viniegra-Gonzalez, G., Deising, H.B., and Aguirre, J. (2007). Phosphopantetheinyl transferase CfwA/NpgA is required for *Aspergillus nidulans* secondary metabolism and asexual development. Eukaryot. Cell **6:** 710–720.

Meister, J., Weber, D., Martino, V., Sterner, O., and Anke, T. (2007). Phomopsidone, a novel depsidone from an endophyte of the medicinal plant *Eupatorium arnottianum.* Z. Naturforsch. C **62:** 11–15.

Mofid, M.R., Finking, R., and Marahiel, M.A. (2002). Recognition of hybrid peptidyl carrier proteins/acyl carrier proteins in nonribosomal peptide synthetase modules by the 4'-phosphopantetheinyl transferases AcpS and Sfp. J. Biol. Chem. **277:** 17023–17031.

Money, N.P., Caesar-TonThat, T.C., Frederick, B., and Henson, J.M. (1998). Melanin synthesis is associated with changes in hyphopodial turgor, permeability, and wall rigidity in *Gaeumannomyces graminis* var. *graminis.* Fungal Genet. Biol. **24:** 240–251.

Mootz, H.D., Schorgendorfer, K., and Marahiel, M.A. (2002). Functional characterization of 4'-phosphopantetheinyl transferase genes of bacterial and fungal origin by complementation of *Saccharomyces cerevisiae lys5.* FEMS Microbiol. Lett. **213:** 51–57.

Neville, C., Murphy, A., Kavanagh, K., and Doyle, S. (2005). A 4'-phosphopantetheinyl transferase mediates non-ribosomal peptide synthetase activation in *Aspergillus fumigatus.* ChemBioChem **6:** 679–685.

Nosanchuk, J.D., and Casadevall, A. (2003). The contribution of melanin to microbial pathogenesis. Cell. Microbiol. **5:** 203–223.

Oberegger, H., Eisendle, M., Schrettl, M., Graessle, S., and Haas, H. (2003). 4'-Phosphopantetheinyl transferase-encoding npgA is essential for siderophore biosynthesis in *Aspergillus nidulans.* Curr. Genet. **44:** 211–215.

Oide, S., Moeder, W., Krasnoff, S., Gibson, D., Haas, H., Yoshioka, K., and Turgeon, B.G. (2006). NPS6, encoding a nonribosomal peptide synthetase involved in siderophore-mediated iron metabolism, is a conserved virulence determinant of plant pathogenic ascomycetes. Plant Cell **18:** 2836–2853.

Panaccione, D.G., Scott-Craig, J.S., Pocard, J.-A., and Walton, J.D. (1992). A cyclic peptide synthetase gene required for pathogenicity of the fungus *Cochliobolus carbonum* on maize. Proc. Natl. Acad. Sci. USA **89:** 6590–6594.

Punt, P.J., Oliver, R.P., Dingemanse, M.A., Pouwels, P.H., and van den Hondel, C.A. (1987). Transformation of *Aspergillus* based on the hygromycin B resistance marker from *Escherichia coli.* Gene **56:** 117–124.

Ramakers, C., Ruijter, J.M., Lekanne Deprez, R.H., and Moorman, A.F.M. (2003). Assumption-free analysis of quantitative real-time polymerase chain reaction (PCR) data. Neurosci. Lett. **339:** 62–66.

Rasmussen, J.B., and Hanau, R.M. (1989). Exogenous scytalone restores appressorial melanization and pathogenicity in albino mutants of *Colletotrichum graminicola.* Can. J. Plant Pathol. **11:** 349–352.

Rohe, M., Gierlich, A., Hermann, H., Hahn, M., Schmidt, B., Rosahl, S., and Knogge, W. (1995). The race-specific elicitor, NIP1, from the barley pathogen, *Rhynchosporium secalis*, determines avirulence on host plants of the *Rrs1* resistance genotype. EMBO J. **14:** 4168–4177.

Sambrook, J., Fritsch, E.F., and Maniatis, T. (1989). Molecular Cloning: A Laboratory Manual. (Cold Spring Harbor, NY: Cold Spring Harbor Laboratory Press).

Sawada, H., Sugihara, M., Takagaki, M., and Nagayama, K. (2004). Monitoring and characterization of *Magnaporthe grisea* isolates with decreased sensitivity to scytalone dehydratase inhibitors. Pest Manag. Sci. **60:** 777–785.

Scheffer, J., Chen, C., Heidrich, P., Dickman, M.B., and Tudzynski, P. (2005). A CDC42 homologue in *Claviceps purpurea* is involved in vegetative differentiation and is essential for pathogenicity. Eukaryot. Cell **4:** 1228–1238.

Schrettl, M., Bignell, E., Kragl, C., Sabiha, Y., Loss, O., Eisendle, M., Wallner, A., Arst, H.N.J., Haynes, K., and Haas, H. (2007). Distinct roles for intra- and extracellular siderophores during *Aspergillus fumigatus* infection. PLoS Pathog. **3:** 1195–1207.

Schweizer, P., Novara, D., and Douchkov, D. (2006). Method for increasing a fungal resistance of transgenic plants by a host-induced suppression of a pathgogenic fungi genetic expression. International Patent Number WO 2006/097465 A2.

Smith, D.B., and Corcoran, L.M. (1994). Expression and purification of gluthathion-S-transferase fusion proteins. In Current Protocols in Molecular Biology, F.M. Ausubel, R. Brent, R.E. Kingston, D.D. Moore, J.G. Seidman, J.A. Smith, and K. Struhl, eds (New York: John Wiley & Sons), pp. 16.17.11.11–16.17.17.

Soid-Raggi, G., Sanchez, O., and Aguirre, J. (2006). TmpA, a member of a novel family of putative membrane flavoproteins, regulates asexual development in *Aspergillus nidulans.* Mol. Microbiol. **59:** 854–869.

Steiner, U., and Oerke, E.C. (2007). Localized melanization of appressoria is required for pathogenicity of *Venturia inaequalis.* Phytopathology **97:** 1222–1230.

Studier, F.W., and Moffatt, B.A. (1986). Use of bacteriophage T7 RNA polymerase to direct selective high-level expression of cloned genes. J. Mol. Biol. **189:** 113–130.

Sugui, J.A., and Deising, H.B. (2002). Isolation of infection-specific sequence tags expressed during early stages of maize anthracnose disease development. Mol. Plant Pathol. **3:** 197–203.

Takeshita, N., Yamashita, S., Ohta, A., and Horiuchi, H. (2006). *Aspergillus nidulans* class V and VI chitin synthases CsmA and CsmB, each with a myosin motor-like domain, perform compensatory functions that are essential for hyphal tip growth. Mol. Microbiol. **59:** 1380–1394.

Treco, D.A., and Lundblad, V. (1993). Basic techniques of yeast genetics. In Current Protocols in Molecular Biology, F.M. Ausubel, R. Brent, R.E. Kingston, D.D. Moore, J.G. Seidman, J.A. Smith, and K. Struhl, eds (New York: John Wiley & Sons), pp. 13.11.11–13.11.17.

Tsuji, G., Kenmochi, Y., Takano, Y., Sweigard, J., Farrall, L., Furusawa, I., Horino, O., and Kubo, Y. (2000). Novel fungal transcriptional activators, Cmr1p of *Colletotrichum lagenarium* and pig1p of *Magnaporthe grisea*, contain Cys2His2 zinc finger and Zn(II)2Cys6 binuclear cluster DNA-binding motifs and regulate transcription of melanin biosynthesis genes in a developmentally specific manner. Mol. Microbiol. **38:** 940–954.

Vernet, T., Dignard, D., and Thomas, D.Y. (1987). A family of yeast expression vectors containing the phage f1 intergenic region. Gene **52:** 225–233.

Walton, J.D. (2006). HC-toxin. Phytochemistry **67:** 1406–1413.

Weiergang, I., Dunkle, L.D., Wood, K.V., and Nicholson, R.L. (1996). Morphogenic regulation of pathotoxin synthesis in *Cochliobolus carbonum.* Fungal Genet. Biol. **20:** 74–78.

Werner, S., Sugui, J.A., Steinberg, G., and Deising, H.B. (2007). A chitin synthase with a myosin-like motor domain is essential for hyphal growth, appressorium differentiation and pathogenicity of the maize anthracnose fungus *Colletotrichum graminicola.* Mol. Plant Microbe Interact. **20:** 1555–1567.

Wilson, R.A., and Talbot, N.J. (2009). Under pressure: Investigating the biology of plant infection by *Magnaporthe oryzae.* Nat. Rev. Microbiol. **7:** 185–195.

Yin, J., Straight, P.D., McLoughlin, S.M., Zhou, Z., Lin, A.J., Golan, D.E., Kelleher, N.L., Kolter, R., and Walsh, C.T. (2005). Genetically encoded short peptide tag for versatile protein labeling by Sfp phosphopantetheinyl transferase. Proc. Natl. Acad. Sci. USA **102:** 15815–15820.

Yu, J.H., Hamari, Z., Han, K.H., Seo, J.A., Reyes-Domínguez, Y., and Scazzocchio, C. (2004). Double-joint PCR: A PCR-based molecular tool for gene manipulations in filamentous fungi. Fungal Genet. Biol. **41:** 973–981.

Zhbanko, M., Zinchenko, V., Gutensohn, M., Schierhorn, A., and Klösgen, R.B. (2005). Inactivation of a predicted leader peptidase prevents photo autotrophic growth of Synechocystis sp strain PCC 6803. J. Bacteriol. **187:** 3071–3078.